

A regulatory network of a piRNA and lncRNA initiates responder and trailer piRNA formation during embryonic development of *Aedes* mosquitoes

Valerie Betting*¹, Joep Joosten*¹, Rebecca Halbach*¹, Melissa Thaler¹, Pascal Miesen¹, and Ronald P. Van Rij¹⁺

¹Department of Medical Microbiology, Radboud Institute for Molecular Life Sciences, Radboud University Medical Center, P.O. Box 9101, 6500 HB Nijmegen, The Netherlands

+ corresponding author: ronald.vanrij@radboudumc.nl

*These authors contributed equally to this study.

ABSTRACT

PIWI-interacting (pi)RNAs are small silencing RNAs that are crucial for the defense against transposable elements in germline tissues of animals. In the mosquito *Aedes aegypti*, the piRNA pathway also contributes to gene regulation in somatic tissues, illustrating additional roles for piRNAs and PIWI proteins besides transposon repression. Here, we identify a highly abundant, endogenous piRNA (propiR1) that associates with both Piwi4 and Piwi5. PropiR1-mediated target silencing requires base pairing in the seed region with supplemental base pairing at the piRNA 3' end. Yet, propiR1 strongly represses a single target, the lncRNA AAEL027353 (lnc027353). Slicing of this target initiates the production of responder and trailer piRNAs from the 3' cleavage fragment. Expression of propiR1 commences early during embryonic development and mediates degradation of maternally provided lnc027353. Both propiR1 and its lncRNA target display a high degree of sequence conservation in the closely related *Aedes albopictus*, underscoring the importance of this regulatory network for mosquito development.

Key words: piRNA, PIWI, long non-coding RNA, *Aedes aegypti*, embryonic development

INTRODUCTION

PIWI proteins are a subfamily of the Argonaute protein family that associate with a specific class of 25-30nt small non-coding RNAs to form RNA-induced silencing complexes (RISCs). These PIWI-interacting (pi)RNAs, akin to small interfering (si)RNAs and micro (mi)RNAs, guide RISCs to cognate RNAs through Watson-Crick base pairing, which results in target silencing (Kobayashi & Tomari, 2016). Whereas biogenesis of miRNAs and siRNAs depends on Dicer-mediated endonucleolytic cleavage of double-stranded precursors, piRNA production is Dicer-independent (Vagin, Sigova et al., 2006).

The piRNA pathway is mostly known for its role in silencing transposons, thus preserving genome integrity in the germline (Czech & Hannon, 2016, Ozata, Gainetdinov et al., 2019). In *Drosophila*, the majority of piRNAs are produced from piRNA clusters, genomic regions that are rich in transposon remnants (Brennecke, Aravin et al., 2007). piRNA cluster transcripts are transported to the cytoplasm, loaded onto the PIWI proteins Aubergine (Aub) and Piwi, and processed into mature piRNAs (Czech & Hannon, 2016, Ozata et al., 2019). Whereas Piwi-piRNA complexes move to the nucleus to guide the deposition of repressive histone marks at transposon loci, piRNA-loaded Aub cleaves target RNAs in the cytoplasm through a mechanism termed slicing, thus repressing transposable elements at the post-transcriptional level (Gunawardane, Saito et al., 2007).

Efficiency of piRNA-mediated silencing relies on processes that amplify and diversify the pool of piRNAs. The 3' cleavage fragments resulting from Aub-mediated slicing are bound by Ago3 and further processed into a responder piRNAs. In turn, Ago3-associated responder piRNAs cleave piRNA cluster transcripts, which are processed into new Aub-associated piRNAs, completing the so-called ping-pong amplification cycle. The preference of Aub to bind piRNAs with a 5' terminal uridine, combined with the fact that PIWI proteins slice their targets between nucleotides 10 and 11 of their guide, gives rise to the 1U/10A ping-pong signature that is characteristic of piRNA production through the ping-pong amplification loop (Gunawardane et al., 2007). The 3' ends of responder piRNAs are defined by the endonuclease Zucchini (Zuc) in complex with accessory proteins at the mitochondrial membrane. In addition, the same complex processes the downstream 3' section of the piRNA precursor into a series of trailer piRNAs (Han, Wang et al., 2015, Mohn, Handler et al., 2015). These trailer piRNAs mainly associate with Piwi and direct transcriptional silencing of transposons in the nucleus.

Although the piRNA pathway is predominantly studied in fruit flies, they represent an atypical case within the arthropod phylum, considering that their piRNA expression is restricted to germline tissues. In most arthropods including *Aedes* mosquitoes, PIWI proteins and piRNAs are expressed in both germline and somatic tissues (Lewis, Quarles et al., 2018). Moreover, the PIWI protein family has undergone expansion to seven members in *Ae. aegypti*, compared to three in *Drosophila* (Campbell, Black et al., 2008, Lewis, Salmela et al., 2016), suggesting that the pathway may have undergone functional diversification in mosquitoes. Indeed, *Aedes* mosquitoes produce piRNAs from a diverse set of substrates and members of the PIWI family show specificity with regard to their piRNA repertoire. For instance, Piwi5 is required for the production of primary transposon-

derived piRNAs and piRNAs derived from endogenous viral elements, whereas Piwi4 is mostly enriched for two piRNAs (tapiR1 and 2) derived from an evolutionary conserved satellite repeat locus, but not for transposon- or virus-derived piRNAs (Halbach, 2020, Miesen, Girardi et al., 2015, Palatini, Miesen et al., 2017, Suzuki, Frangeul et al., 2017, Whitfield, Dolan et al., 2017). Additionally, Piwi5 and Ago3 are the core proteins in the ping-pong amplification loop that produces piRNAs from viral, transposon and messenger RNA substrates (Arensburger, Hice et al., 2011, Girardi, Miesen et al., 2017, Joosten, Miesen et al., 2019, Miesen et al., 2015).

The observation that *Ae. aegypti* produces abundant piRNAs mapping to protein-coding genes strongly suggest that the piRNA response in *Aedes* mosquitoes extends to gene regulation (Arensburger et al., 2011, Girardi et al., 2017, Miesen et al., 2015). Indeed, we recently demonstrated that the Piwi4-associated piRNA tapiR1 regulates the expression of both protein-coding and non-coding RNAs. Moreover, selective inhibition of tapiR1 disrupted embryonic development, illustrating the importance of piRNA-mediated gene regulation during development (Halbach, 2020). piRNAs have also been shown to regulate gene expression in other species. For example, pachytene piRNAs expressed from non-transposon intergenic regions, mediate the degradation of specific mRNAs and long non-coding RNAs (lncRNAs) during mouse spermatogenesis (Watanabe, Cheng et al., 2015).

piRNA-mediated gene regulation has been shown to be crucial in the embryonic development of both fruit flies and mosquitoes (Halbach, 2020, Rouget, Papin et al., 2010, Vourekas, Alexiou et al., 2016). Early embryonic development of animals is driven by maternally provided mRNAs until maternal-to-zygotic transition (MZT), during which the zygotic genome is activated and maternal mRNAs are degraded (Tadros & Lipshitz, 2009). Degradation of maternal mRNAs relies, at least in part, on maternally deposited piRNAs in fruit flies (Barckmann, Pierson et al., 2015, Rouget et al., 2010), and on zygotic piRNAs in *Aedes* mosquitoes (Halbach, 2020).

To further dissect the gene regulatory potential of individual endogenous *Ae. aegypti* piRNAs, we describe here a highly abundant, Piwi4- and Piwi5-associated piRNA that we named propiR1. We found that this piRNA strongly silences a single target: the lncRNA AAEL027353 (lnc027353). propiR1 expression commences during the first hours of embryonic development to direct the degradation of lnc027353, suggesting that this regulatory network is important for embryonic development.

RESULTS

A host-derived piRNA associates with Piwi4 and Piwi5

To evaluate the gene regulatory potential of the *Ae. aegypti* piRNA pathway, we inspected small RNA deep-sequencing data from *Ae. aegypti*-derived Aag2 cells to find highly abundant piRNAs. We focused on Piwi5-associated piRNAs, as Piwi5 is initially loaded with primary piRNAs from endogenous sources and engages in efficient feed forward piRNA amplification through the ping-pong loop (Joosten et al., 2019, Miesen et al., 2015). To identify endogenous piRNAs with putative gene regulatory potential, we selected the top 25 most

abundant Piwi5-associated piRNAs in Aag2 cells using previously published small RNA data from PIWI immunoprecipitations (IP) (Miesen et al., 2015). Strikingly, the Piwi5-associated piRNA with the highest expression in Aag2 cells does not map to transposon sequences (Figure 1A), and we set out to investigate this piRNA further.

Upon closer inspection, we found that this piRNA was expressed as two distinct isoforms of 27 and 30 nt in size (Supplementary Figure 1A). Small RNA deep sequencing as well as northern blotting revealed that both isoforms were enriched in Piwi5-IP, yet, the 30-nt isoform specifically interacted with Piwi4 (Figure 1B-C, Supplementary Figure 1B). This specific Piwi4-enrichment was missed in the initial analysis, as we did not examine piRNA enrichment for the distinct sizes separately. Because of this dual PIWI protein association pattern, we named this piRNA: promiscuous piRNA 1 (propir1).

Next, we investigated the involvement of different PIWI proteins in propir1 biogenesis, by assessing the effect of RNAi-mediated knockdown of Ago3 and Piwi4-6, as these PIWI genes are abundantly expressed in germline and somatic mosquito tissues as well as the somatic Aag2 cell line (Akbari, Antoshechkin et al., 2013, Joosten et al., 2019, Vodovar, Bronkhorst et al., 2012). In accordance with the differential association of the two propir1 isoforms, Piwi4 knockdown resulted in a mild reduction of the larger 30-nt isoform, while abundance of the 27-nt isoform was clearly reduced upon Piwi5 knockdown (Figure 1D).

Interestingly, we found that Piwi4 knockdown resulted in an increased abundance of the short propir1 isoform, suggesting an interplay between Piwi4 and Piwi5 in propir1 biogenesis. We propose that competition between Piwi4 and Piwi5 for a putative propir1 precursor may account for the divergent effects of PIWI knockdown on propir1 biogenesis. As expected, knockdown of

Ago1 and Ago2, components of the miRNA and siRNA pathway respectively, did not affect biogenesis of either propir1 isoform (Figure 1D).

After loading onto PIWI proteins and subsequent maturation, piRNA 3' ends are 2'-O-methylated by the S-adenosylmethionine (SAM)-dependent methyltransferase Hen1 (Horwich, Li et al., 2007, Saito, Sakaguchi et al., 2007, Tian, Simanshu et al., 2011). The presence of this modification can be assessed by sodium periodate oxidation followed by β -elimination, resulting in the removal of the 3' terminal nucleoside and increased electrophoretic mobility of unmodified RNAs (Kawaoka, Katsuma et al., 2014). In contrast to the miRNA miR2940-3p, both propir1 isoforms are unaffected by β -elimination (Figure 1E), indicating that these piRNAs have 2'-O-methylated 3' ends and are mature, PIWI protein associated piRNAs. Moreover, these results suggests that the 30-nt isoform is unlikely a precursor of the 27-nt isoform.

propir1 piRNAs mapped to seven locations on chromosome 3 (Figure 1F), five of which are inside piRNA clusters (as annotated in Crava et al, in prep.). These seven sites displayed a high degree of sequence conservation covering the piRNA and a ~250 bp flanking sequence element (Figure 1G). The sequence outside this element was more divergent, suggesting that the piRNA site was duplicated on the chromosome as part of a larger fragment, of which the ~250 nt sequence element was preferentially maintained throughout evolution.

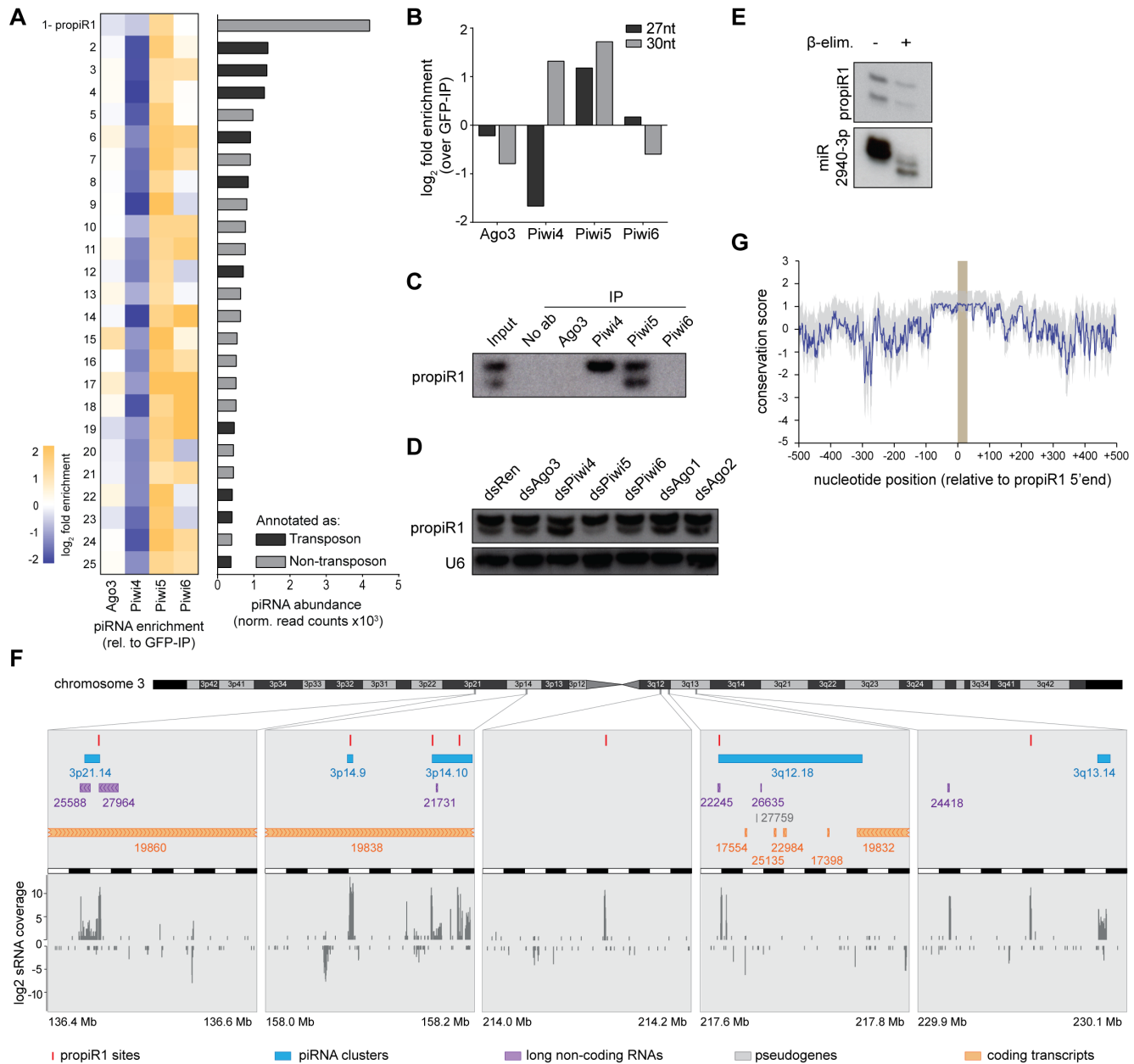


Figure 1. The endogenous piRNA propiR1 has two isoforms that differentially associate with Piwi4 and Piwi5.

A) Ranked list of the top-25 most abundant piRNAs in a Piwi5 immunoprecipitation (IP) in Aag2 cells. The heatmap (left) represents piRNA-enrichment in different PIWI protein IP libraries; the bar chart (right) shows piRNA abundance in Aag2 cells. Dark gray bars indicate transposon-derived piRNAs; light gray bars indicate piRNAs not mapping to annotated transposons.

B) Enrichment of the two most abundant propiR1 isoforms (27 and 30nt) in PIWI protein IP small RNA sequencing libraries.

C) Northern blot analysis of propiR1 enrichment in PIWI protein IPs using antibodies targeting endogenous PIWI proteins from Aag2 cell lysates. An IP in which the antibody was omitted serves as control (No ab).

D) Northern blot analysis of propiR1 in Aag2 cells transfected with dsRNA targeting the indicated genes, and *Renilla* luciferase (dsRen) as a control. U6 snRNA serves as loading control.

E) Northern blot analysis of propiR1 and miR-2940-3p in RNA samples subjected to β -elimination as indicated. The blot was reused from (Halbach, 2020) and re-probed for propiR1. The miR2940-3p panel is shown here again as a control.

F) Schematic representation of propiR1 sites on chromosome 3 of *Ae. aegypti* and their piRNA coverage. propiR1 sites are indicated in red. Protein-coding genes, pseudogenes and piRNA clusters (as annotated in VectorBase) in a 200 kb window flanking the propiR1 piRNA sites are color-coded as indicated. piRNA clusters (in blue) were named according to chromosomal location, as described in (Crava et al., in prep). VectorBase gene identifiers (without the AAEL0 species prefix) were used to refer to transcripts. Small RNA coverage in Aag2 cells is indicated relative to 10^6 miRNAs.

G) Sequence conservation between the seven propiR1 sites (marked as a gray box) and 500bp flanking regions. The conservation scores (solid purple line) and 50% confidence intervals (gray shading) are indicated for each nucleotide position.

prop1R1 is able to silence target RNAs in trans

Studies in *Ae. aegypti* and *C. elegans* have shown that piRNAs silence mRNAs via miRNA-like recognition using a 5' seed sequence (nt 2-7) with additional 3' supplementary base pairing (Halbach, 2020, Shen, Chen et al., 2018). To evaluate *prop1R1* silencing potential and targeting requirements, we set up a reporter assay in which a single 30nt target site for *prop1R1* was introduced into the 3' UTR of firefly luciferase (FLuc) (Figure 2A). This reporter thus contains a fully complementary target site for both the 27-nt and 30-nt isoforms. Compared to a reporter without a target site, the reporter bearing a fully complementary *prop1R1* target site was silenced ~10-fold (Figure 2B). To assess *prop1R1* targeting requirements, we introduced a series of mismatches in the target sequence of the FLuc reporter (Supplementary Figure 2). As anticipated, introduction of three consecutive mismatches in the target sequence expected to base pair with nt 1-9 of *prop1R1* (t1-9) resulted in strong desilencing of the reporter (Figure 2C, dark blue bars). Moreover, single nucleotide mismatches introduced at positions t2-8 resulted in partial desilencing of the reporter (Figure 2C, light blue bars). A mismatch at position t1 did not affect reporter silencing (Figure 2C), which fits the observation that piRNA 5' ends are tightly anchored in the binding pocket in the MID-domain of PIWI proteins (Matsumoto, Nishimasu et al., 2016, Yamaguchi, Oe et al., 2020) and therefore do not contribute to target recognition. Argonaute family proteins with slicing activity cleave their target RNAs between nucleotides 10 and 11. Introducing a single mismatch at t10 or three consecutive mismatches at t10-12, which covers the putative slice site, did not result in strong desilencing (Figure 2C), suggesting either that a slicing-independent mechanism is responsible for *prop1R1*-mediated silencing, or that base pairing at the slice site is dispensable for slicing.

Introduction of an increasing number of mismatches in the target RNA corresponding to the piRNA 3' end resulted in gradual desilencing of the reporter (Figure 2C, yellow bars). Abolishing 3' supplementary pairing altogether (mut t13-30) resulted in almost complete desilencing of the reporter, indicating that seed-based target recognition alone is not sufficient for *prop1R1*-mediated silencing and that additional 3' supplemental base pairing is essential. Altogether, our results establish nt 2-8 as the seed region of *prop1R1*, at which base pairing is required for efficient targeting. Yet, seed-based target recognition is not sufficient for *prop1R1*-mediated silencing and 3' supplemental base pairing is essential.

To analyze PIWI protein dependency of reporter silencing, we performed a reporter assay in the context of knockdown of the PIWI genes that are expressed in Aag2 cells. As a control, we transfected cells with dsRNA targeting GFP (dsGFP), in which the reporter bearing the *prop1R1* target site was silenced ~20-fold (Figure 2D). Reporter silencing is reduced most prominently upon knockdown of *Piwi5* (~4.5-fold reduction compared to the control, dsRNA targeting GFP; Figure 2D). Yet, minor desilencing is also observed upon knockdown of *Ago3* (~1.7-fold reduction) and *Piwi6* (~1.8-fold reduction). Surprisingly, knockdown of *Piwi4* resulted in more efficient reporter silencing (~2-fold; Figure 2D). This might be due to competition between *Piwi4* and *Piwi5* for the putative *prop1R1* precursor and increased levels of the short, *Piwi5*-associated *prop1R1* isoform upon *Piwi4* knockdown (Figure 1D). We hypothesize that silencing of the reporter bearing a fully complementary target

site is largely mediated by Piwi5 and that knockdown of Piwi4 increases propiR1 loading onto Piwi5, leading to more robust Piwi5-mediated silencing.

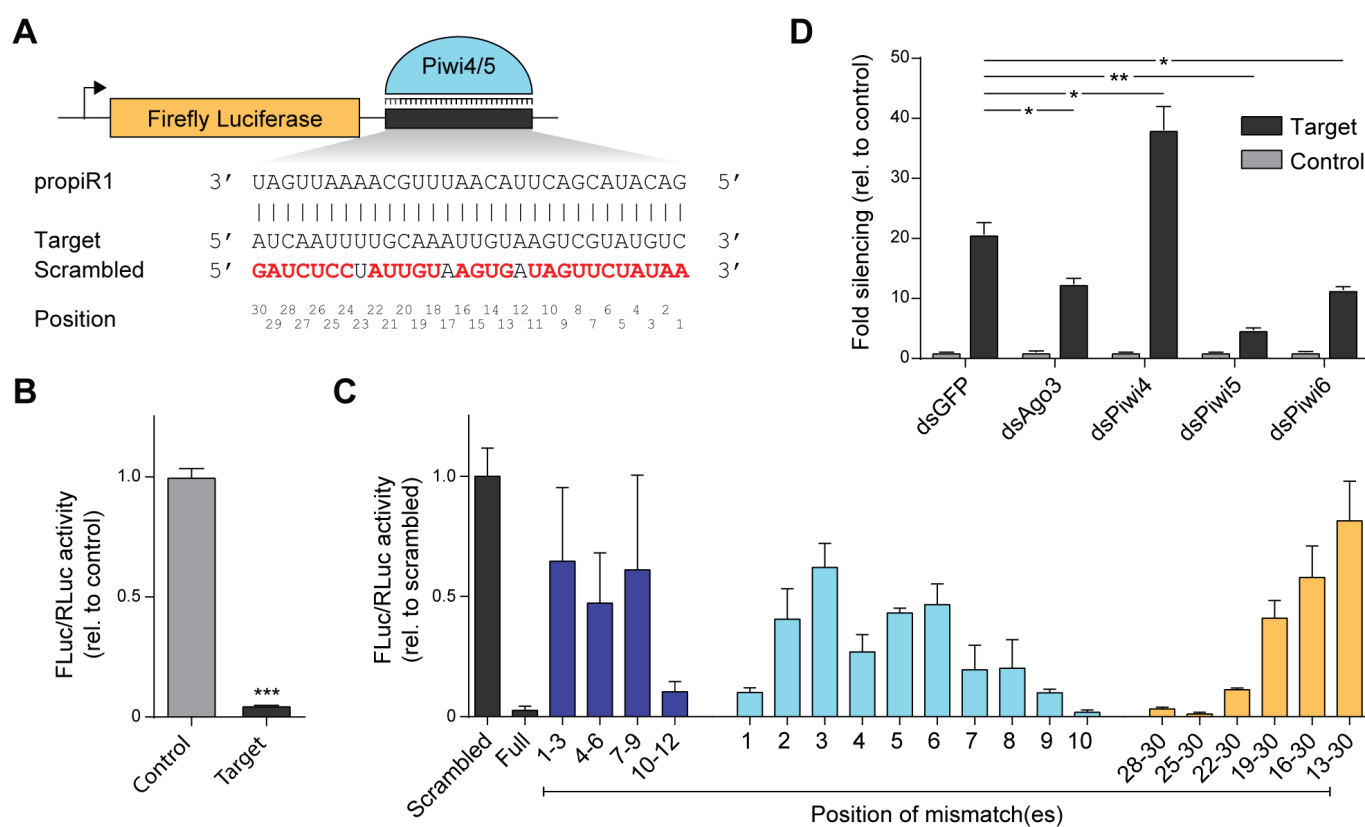


Figure 2. propiR1 has gene regulatory potential *in trans*.

A Schematic representation of the firefly luciferase (FLuc) reporters bearing a propiR1 target site or a control sequence in the 3' UTR. Numbers correspond to the position of residues in the target RNA (t1-30) that are opposite propiR1 nucleotides 1-30 (from 5' to 3'). Sequences of propiR1, a fully complementary target site, and the scrambled control (used in (C)) are shown.

B Luciferase assay using reporters bearing a fully complementary target site (Target) or no target site (Control). FLuc activity was normalized to a co-transfected *Renilla* luciferase (RLuc) reporter [same in (C) and (D)]. Bars represent mean \pm standard deviation of a representative of five independent experiments, each measured using biological triplicates. *** $P < 0.0005$ (unpaired t-test).

C Luciferase assay of reporters with propiR1 target sites harboring three consecutive mismatches (dark blue) or single nt mismatches (light blue), or an increasing number of mismatches corresponding to the 3' end of the piRNA (yellow). Numbers indicate positions in the target site (t1-30 – shown in (A)) that were mutated. In all cases, guanosine residues were changed to cytidine, adenosine to uridine, and *vice versa*. Bars depict mean \pm standard deviation of a representative of three independent experiments, each performed with three biological replicates.

D Luciferase assay using reporters with either a fully complementary target site (Target) or no target site (Control) upon PIWI gene knockdown in Aag2 cells. dsRNA targeting GFP (dsGFP) was used as a control. Data are mean \pm standard deviation of a representative of three independent experiments, each with three biological replicates. Asterisks denote statistically significant differences in fold silencing between dsGFP control and PIWI gene knockdowns (unpaired two tailed t-tests with Holm-Sidak correction; * $P < 0.05$, ** $P < 0.005$).

propiR1* regulates expression of *Inc027353

To validate that reporter silencing was indeed mediated by propiR1, we designed 2'-O-methylated antisense RNA oligonucleotides (AOs) fully complementary to propiR1 that are expected to inhibit propiR1-mediated target silencing. Treatment with propiR1 AOs resulted in reduced levels of both propiR1-isoforms (Supplementary Figure 3A). In a luciferase assay in which cells were transfected with increasing concentrations of AOs, reporter silencing was abolished in a concentration-dependent manner, confirming that reporter silencing was indeed propiR1-dependent (Figure 3A).

To identify endogenous transcripts targeted by propiR1, we compared the transcriptomic landscape of Aag2 cells treated with propiR1 AOs to that of cells treated with control AOs using RNA-seq (Figure 3B). propiR1 AO treatment resulted in a ~7.7-fold increase of a single lncRNA (AAEL027353, referred to as lnc027353 throughout this study, $P = 2.9E-64$), while a handful of other lncRNAs and mRNAs were mildly affected as well (Figure 3B). Furthermore, expression of transposon mRNAs was unaffected by propiR1 AO treatment (Supplementary Figure 3B).

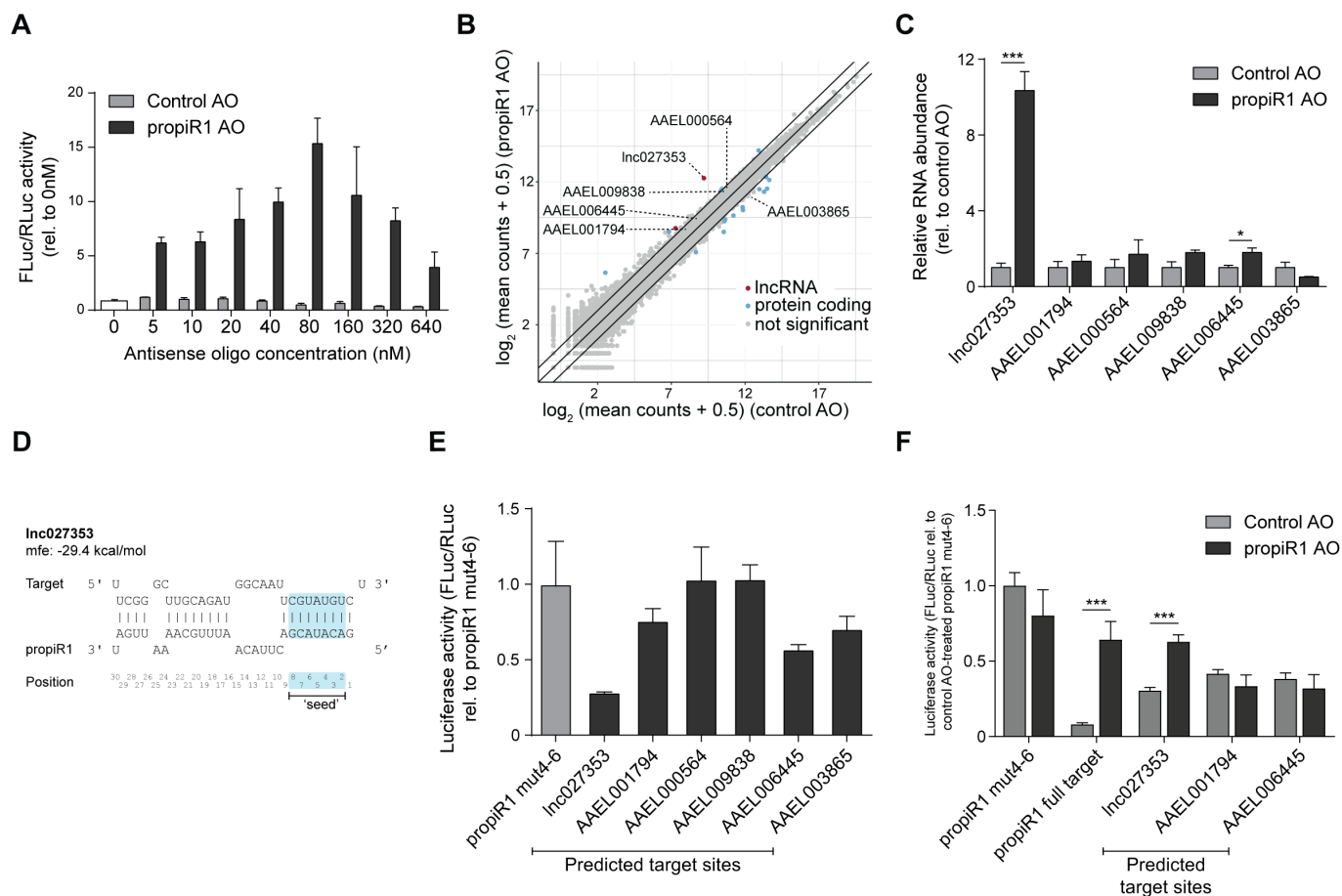


Figure 3. propiR1 regulates a limited set of cellular RNAs.

A Luciferase assay using a firefly luciferase (FLuc) reporter bearing a fully complementary propiR1 target site in the 3'UTR. Increasing amounts of 2'-O-methylated RNA antisense oligonucleotides for propiR1 (prop*i*R1 AO) or a control sequence (control AO) were co-transfected with the propiR1 reporter plasmid. FLuc activity was normalized to the activity of a co-transfected *Renilla* luciferase (RLuc) reporter [same in (E) and (F)]. Bars show the mean \pm standard deviation of a representative of two independent experiments, each measured in triplicate.

B \log_2 gene expression in Aag2 cells treated with propiR1- or control AOs. Mean RNA-seq counts of three biological replicates are shown (plus a pseudo-count of 0.5 to plot values of zero). Significance was tested at an FDR of 0.01 and \log_2 fold change of 0.5. Diagonal lines highlight a 2-fold change. Significantly differentially expressed lncRNAs and protein coding genes are indicated with red and blue dots, respectively; gray dots indicate genes that were not significantly affected by propiR1 AO treatment.

C RT-qPCR of genes bearing propiR1 target sites after treatment with propiR1 or control AOs for 24 hours. Shown are the mean \pm standard deviation of a representative of three independent experiments, measured using biological triplicates. Asterisks denote statistically significant differences in gene expression between propiR1 and control AO treated cells (unpaired two tailed t-tests with Holm-Sidak correction; *** $P < 0.0005$).

D Schematic representation of the predicted propiR1-lnc027353 duplex and its minimum free energy (mfe). Numbers indicate propiR1 piRNA positions (5' to 3') with the seed sequence (nt 2-8) in blue shading.

E Luciferase assay of reporters containing predicted propiR1 target sites from genes differentially expressed upon propiR1 AO treatment. Depicted are the mean \pm standard deviation of a representative of three independent experiments, each with three biological replicates.

F Luciferase assay of reporters containing predicted propiR1 target sites upon co-transfection with propiR1 or control AOs. Bars represent the mean \pm standard deviation of four biological replicates. Asterisks denote statistically significant desilencing upon treatment with propiR1 AOs (unpaired two tailed t-tests with Holm-Sidak correction; *** $P < 0.0005$).

We used RNAHybrid (Rehmsmeier, Steffen et al., 2004) to predict propiR1 target sites in affected genes (Supplementary Figure 3C). Besides Inc027353, none of the significantly affected genes contained predicted propiR1 target sites. Hence, we selected the most strongly (albeit not significantly) affected genes bearing propiR1 target sites and evaluated their altered expression upon propiR1 AO treatment using RT-qPCR (Figure 3C). While most changes in expression were mild and not significant, Inc027353 expression was strongly increased (~10.3-fold) upon propiR1 AO treatment (Figure 3C), akin to what we found using RNA-seq (Figure 3B). Additionally, we analyzed one gene that was downregulated ~2.1-fold in propiR1 AO-treated cells in RNA-seq (AAEL003865) and were able to confirm this reduction (Figure 3C), further validating our RNA-seq results.

To evaluate whether the changes in expression were due to direct propiR1-mediated targeting of these transcripts, we introduced the predicted target sites into the 3'UTR of FLuc reporters (Figure 3D, Supplementary Figure 3C). Four out of six of the predicted target sites induced reporter silencing to some extent, of which the reporter containing the Inc027353 target site was silenced most efficiently (~3.5-fold; Figure 3E). Luciferase activity of the reporter containing the AAEL003685 target site was not increased (Figure 3E), indicating that the reduction in AAEL003685 expression upon selective propiR1 inhibition of is likely an indirect, yet PIWI-gene dependent effect (Supplementary Figure 4).

To test whether the reporters with predicted target sites are specifically silenced by propiR1, we co-transfected the FLuc reporters with propiR1 or control AOs. Only the reporter bearing the predicted target site from Inc027353, but not from AAEL001794 and AAEL006445, was silenced upon co-transfection of propiR1 AOs (Figure 3F). propiR1 binds the Inc027353 target through fully complementary base pairing at the seed region (nt2-9), followed by a large bulge including position 10 and 11 (RNAHybrid did not predict adenine-uridine base pairing at position 11 and 12), supplemented with incomplete base pairing at the 3' end (Figure 3D). Among the tested target sites, the predicted propiR1-target duplex in Inc027353 had the lowest minimum free energy among (-29.4, kcal/mol, Figure 3D, Supplementary Figure 3C), suggesting that binding efficiency affects the level of target silencing. Together, these results indicate that propiR1 efficiently and directly silences Inc027353 through a partially complementary target site.

Piwi4 and Piwi5 cooperatively regulate Inc027353 expression

To dissect the contribution of the propiR1-associated PIWI proteins to silencing of endogenous targets, we performed Piwi4 and Piwi5 single and double knockdowns. In line with our previous findings (Figure 1D), knockdown of Piwi4 resulted in lower levels of the 30-nt isoform, and increased abundance of the Piwi5-bound 27-nt isoform (Figure 4A). Conversely, Piwi5 knockdown lead to reduced levels of both propiR1-isoforms, whereas combined knockdown of Piwi4 and Piwi5 resulted in an even more pronounced reduction of both propiR1 isoforms (Figure 4A).

To further examine the contribution of individual PIWI proteins to propiR1-mediated target silencing, we performed luciferase assays using reporters bearing different propiR1 target sites in the context of single and

double knockdown of Piwi4 and Piwi5. As shown previously (Figure 2D), silencing of a reporter bearing a fully complementary target site is partially alleviated by Piwi5 knockdown (~3.5 fold desilencing; Figure 4B), whereas Piwi4 knockdown increased reporter silencing (~2-fold; Figure 4B). In contrast, Piwi4 knockdown resulted in desilencing of a reporter bearing the endogenous target site from Inc027353 (2~fold desilencing, Figure 4B), which was not affected by knockdown of Piwi5. Together, these data suggest that Piwi5 requires extensive base-pairing to achieve target silencing, whereas Piwi4 predominantly silences its targets through partial base-pairing.

Next, we evaluated the effects of PIWI gene knockdown on expression of the endogenous propiR1 target Inc027353. Piwi4 and Piwi5 single knockdown resulted in a 10-fold and ~4-fold increase in Inc027353 expression, respectively (Figure 4C). Knockdown of both Piwi4 and Piwi5 together resulted in a further increase of Inc027353 expression (~17-fold, Figure 4C), suggesting that target silencing is achieved in a cooperative fashion between these two PIWI proteins. While Piwi5-KD resulted in a moderately increased Inc027353 expression (Figure 4C), luciferase activity of a reporter bearing the Inc027353 target site was unaffected by Piwi5-KD (Figure 4B). This discrepancy may be explained by differences in sensitivity between the two assays. Alternatively, Piwi5 might be able to engage the propiR1 target site only in the context of the native transcript, due to sequence constraints outside the target site itself.

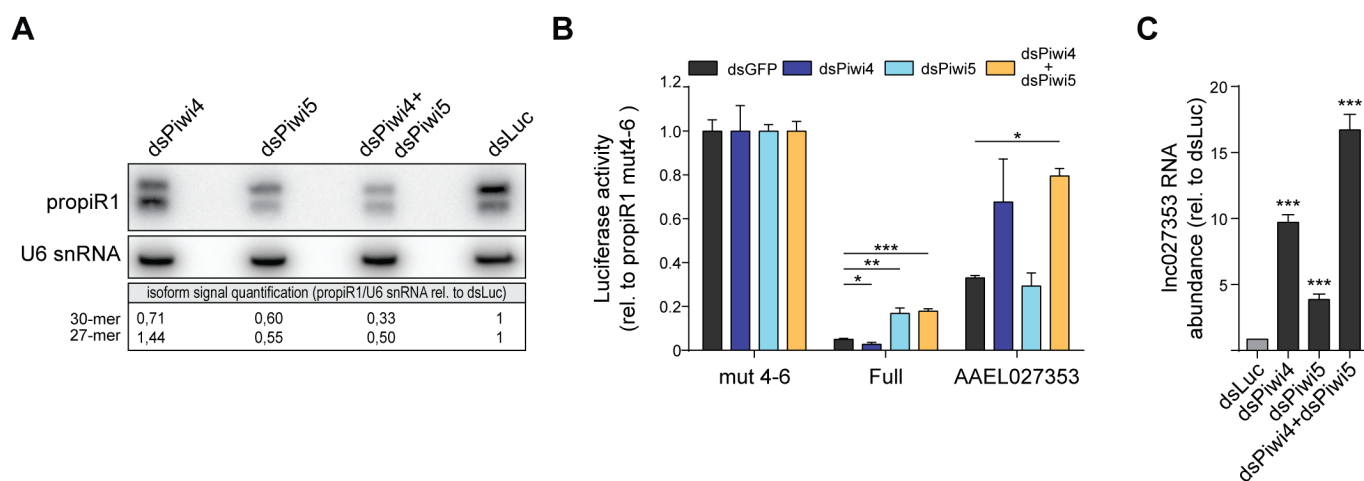


Figure 4. Piwi4 and Piwi5 adhere to different targeting rules.

A) Northern blot analysis comparing the levels of the two propiR1 isoforms in Piwi4 and Piwi5 single and double knockdown to a control knockdown (dsLuc). U6 snRNA serves as a loading control. The numbers below the blot are the quantified signal for each of the individual propiR1 isoforms, normalized to the U6 loading control, with the dsLuc control knockdown set to 1.

B) Luciferase assay of reporters bearing a fully complementary propiR1 target (full), or the endogenous target site of Inc027353 after single or double knockdown of Piwi4 and Piwi5. A propiR1 target site in which residues t4-6 were mutated (mut 4-6) serves as control. Luciferase activity was normalized to the mut4-6 control treated with the same dsRNA. Shown is a representative of three independent experiments, each with three biological replicates. Asterisks indicate statistically significant desilencing of indicated reporters upon PIWI-gene knockdown compared to the dsGFP-treatment (unpaired two tailed t-tests with Holm-Sidak correction; * $P < 0.05$, ** $P < 0.005$, *** $P < 0.0005$).

C) Relative expression of the propiR1 target gene Inc027353 upon Piwi4 and Piwi5 single and double knockdown in Aag2 cells, measured by RT-qPCR. dsLuc knockdown serves as a control and was used in single knockdowns to equalize the total amount of dsRNA per condition. Data represent the mean and standard deviation of three biological replicates. Asterisks indicate statistically significant differences in Inc027353 expression compared to dsLuc (unpaired two tailed t-tests with Holm-Sidak correction; *** $P < 0.0005$).

***propir1* targeting initiates production of *Inc027353*-derived responder and trailer piRNAs**

PIWI protein-mediated slicing may trigger the production of responder and trailer piRNAs through ping-pong amplification and phased piRNA biogenesis, respectively (Gunawardane et al., 2007, Han et al., 2015, Mohn et al., 2015). Upon close inspection of small RNAs mapping to *Inc027353*, we found that the *IncRNA* transcript is indeed processed into responder and trailer piRNAs (Figure 5A). Despite the fact that *propir1* and the *Inc027353* target site do not base pair at position t10/11 (Figure 3D), we found ample production of responder piRNAs with a 5'-5' offset of 10nt respective to *propir1* that is generated from the *IncRNA* cleavage fragment (Figure 5A). Furthermore, we detected low levels of trailer piRNAs generated from the *Inc027353* transcript, downstream of the *propir1* target site. Treating cells with *propir1* AOs, which reduce the expression of both *propir1* isoforms (Figure 4A), abolished production of the *Inc027353*-derived responder piRNA (Figure 5B), indicating that production of the responder piRNA is directly dependent on *propir1*-mediated targeting. As *Piwi5* and *Ago3* are the core proteins in the ping-pong amplification complex, they are considered to have slicing activity (Joosten et al., 2019, Miesen et al., 2015). *Piwi4*, on the other hand, regulates gene expression independent of slicing activity, at least in the context of *tapiR1* (Halbach, 2020). The production of *Inc027353*-derived responder piRNAs suggests that *propir1*-loaded *Piwi5* slices the *Inc027353* target RNA despite the bulge in its target site. Indeed, the *Inc027353*-derived responder piRNA was present in *Ago3*-IP material (Figure 5C), suggesting that it is produced through a *Piwi5* and *Ago3*-mediated ping-pong amplification loop.

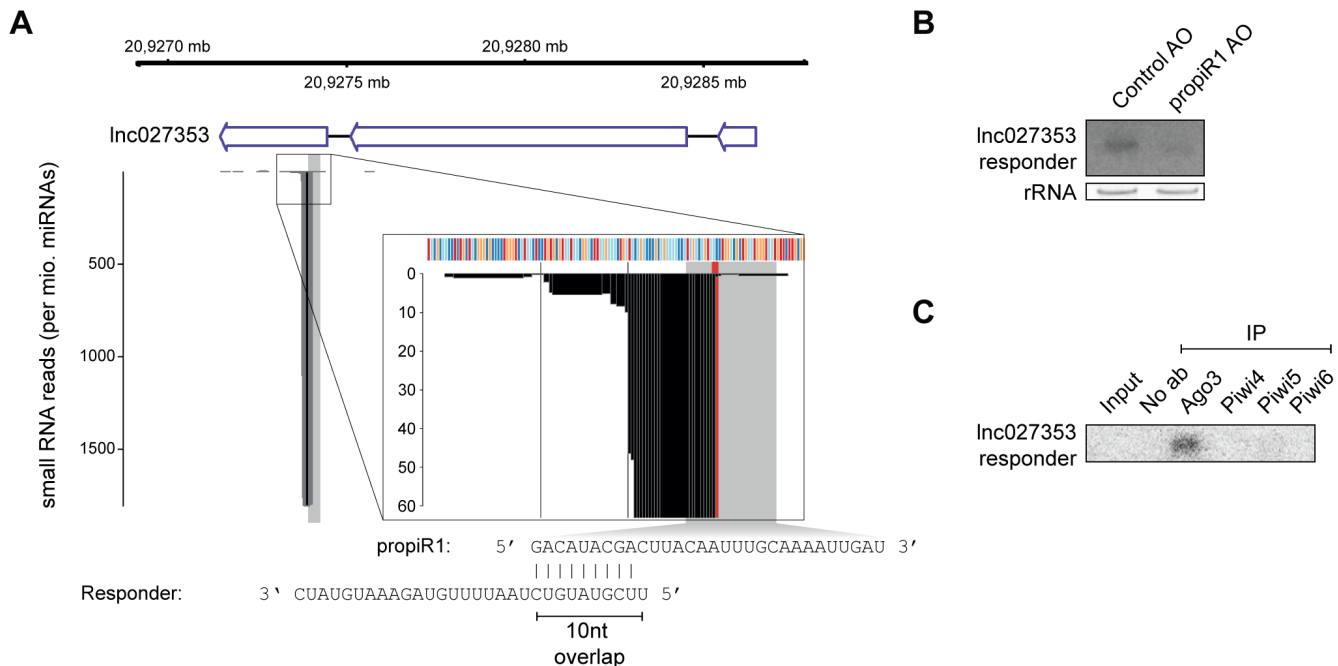


Figure 5. *propir1* targeting of *Inc027353* initiates responder and trailer piRNA production.

A) Genomic coordinates and annotation of the *Inc027353* locus (top). Depicted below is the small RNA coverage of the locus, with the position of the *propir1* target site indicated with a gray box. A magnification on the y-axis and x-axis is shown in the inset. The putative slice site (t10/11) is highlighted in red. Black lines indicate distances of 30 nt from the putative slice site. The genomic sequence of the locus is represented with colored boxes (red: G; orange: C; light blue: A; dark blue: T). The sequence of *propir1* and the AEL027353-derived responder piRNA are shown at the bottom.

B) Northern blot analysis of the *Inc027353*-derived responder piRNA in cells treated with *propir1* or control antisense oligonucleotides (AO). EtBr stained rRNA serves as a loading control.

C) Northern blot analysis of the *Inc027353*-derived responder piRNA in RNA extracted from immunoprecipitations (IP) of the indicated PIWI proteins. No ab indicates a control IP in which the antibody was omitted.

The propiR1-controlled regulatory network is evolutionarily conserved

AAEL027353 is annotated in VectorBase as a ~1.3 kb lncRNA containing two introns (Figure 6A). However, publicly available RNA sequencing data (Akbari et al., 2013) suggest that only a small fraction (~300 bp) is transcribed, which includes parts of exons 2 and 3 and contains the propiR1 target site (Figure 6A). Using RT-PCR, we validated expression of the exon2-3 junction, as well as splicing of the intervening intron (Supplementary Figure 5A). Strikingly, the transcribed region of lnc027353 coincides with an area of high conservation between *Ae. aegypti* and *Ae. albopictus* (Figure 6A; Supplementary Figure 5B). This prompted us to investigate whether the regulatory circuit of propiR1 and lnc027353 is conserved in *Ae. albopictus*.

prop*iR1* is highly abundant in *Ae. albopictus* U4.4 cells, however, unlike *Ae. aegypti* prop*iR1*, *Ae. albopictus* prop*iR1* is almost exclusively expressed as a 29-mer, with only a small fraction being 28nt in size (Figure 6B). The shorter isoform was absent in Piwi5 knockout (KO) U4.4 cells (Figure 6C) [description and characterization of Piwi5 KO cells in (Varghese et al, in prep)], suggesting that, as in *Ae. aegypti*-derived Aag2 cells, the shorter isoform exclusively associates with Piwi5. In contrast, the longer 29nt prop*iR1* isoform is abundantly present in Piwi5 KO cells (Figure 6C), indicating that its production does not require Piwi5, but is likely Piwi4 dependent.

Using the previously established luciferase assays, we found that the reporter bearing a target site fully complementary to *Ae. aegypti* prop*iR1* (containing a single mismatch to *Ae. albopictus* prop*iR1*; Supplementary Figure 5C-upper panel) is efficiently silenced in WT U4.4 cells (~4-fold, Figure 6D). This silencing is partially alleviated in two independent Piwi5 KO U4.4 cell lines (<2-fold, Figure 6D), suggesting that in *Ae. albopictus*, Piwi4 and Piwi5 cooperatively silence this reporter.

The prop*iR1* target site is largely conserved in the *Ae. albopictus* ortholog of lnc027353 and is predicted to be targeted through seed- and supplementary base pairing at the 3' end (Supplementary Figure 5B, C-lower panel). Luciferase activity of a reporter bearing the lnc027353 target site is comparable between Piwi5-KO and WT cells (Figure 6D), indicating that silencing of this partially complementary target site is independent of Piwi5, and instead likely mediated by Piwi4.

To confirm prop*iR1*-mediated regulation of the lncRNA in *Ae. albopictus* cells, we transfected prop*iR1* AOs into Piwi5 KO and WT U4.4 cells. We found that expression of the lnc027353-orthologue was increased ~16-fold in WT U4.4 cells and ~13-fold in a clonal CRISPR control U4.4 cell line upon prop*iR1* AO treatment (Figure 6E), indicating strong prop*iR1*-mediated regulation. In prop*iR1* AO treated Piwi5-KO cells, lncRNA expression increased even more dramatically (~39–55-fold; Figure 6E). These results indicate that *Ae. albopictus* orthologue of lnc027353 is silenced in a Piwi5 independent, presumably Piwi4 dependent manner. Interestingly, within the conserved orthologue of lnc027353, the prop*iR1* target site and the downstream sequence shows a higher degree of sequence similarity compared to the rest of the transcript (Supplementary Figure 5B). Hence, the regulatory circuit based on prop*iR1* and its lncRNA target is highly conserved between different *Aedes* species, underlining its evolutionary importance.

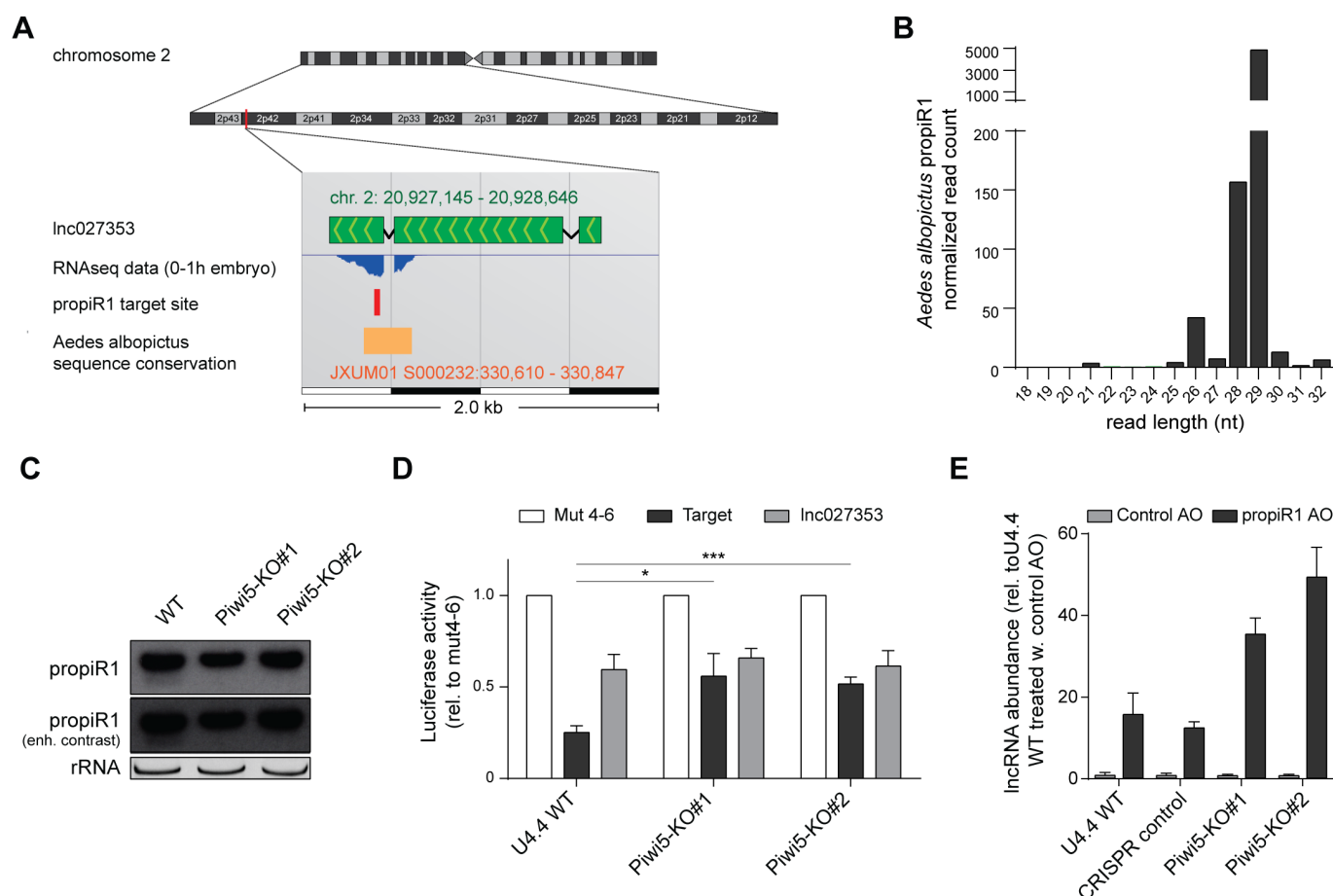


Figure 6. The propiR1- Inc027353 regulatory network is evolutionarily conserved.

A) Schematic representation of the genomic location of Inc027353 on *Ae. aegypti* chromosome 2 obtained from VectorBase. RNA-seq data from 0-1 h embryos (published under SRA accession SRS282183) are displayed using the APOLLO genome browser accessible through VectorBase. The position of the propiR1 target site and an area with high degree of sequence conservation to *Ae. albopictus* are indicated.

B) Size distribution of propiR1-isoforms in *Ae. albopictus*. The read count is normalized to library size.

C) Northern blot analysis of propiR1 in wildtype (WT) and two Piwi5 knockout clones (KO) of *Ae. albopictus*-derived U4.4-cells. The middle panel shows the propiR1 signal after contrast was adjusted to enhance the signal for the short propiR1 isoform. EtBr stained rRNA serves as loading control.

D) Luciferase assay in WT and Piwi5 KO U4.4 cells using reporters containing a control target site with mismatches at positions t4-6 (Mut 4-6), a fully complementary propiR1 target site (Target) or the endogenous target site from *Ae. aegypti* Inc027353. Fold-silencing relative to mut 4-6 is shown. Data were normalized to the activity of a co-transfected RLuc reporter [same in (E)]. Bars and whiskers represent the mean \pm standard deviation of three independent experiments, each measured using biological triplicates. Asterisks mark significant changes in luciferase activity between the different cell lines transfected with the same reporter (unpaired two tailed t-tests with Holm-Sidak correction; * $P < 0.05$, *** $P < 0.0005$).

E) Expression of the Inc027353 orthologue in *Ae. albopictus* U4.4 cells, measured by RT-qPCR, after treatment with 300nM propiR1 or control AOs for 48 hours. CRISPR control is a clonal control cell line generated in parallel with the Piwi5 KO cell lines. Bars and whiskers depict the mean and standard deviation of three biological replicates.

The propiR1- Inc027353 regulatory circuit is active in vivo

Inc027353 is expressed in all tissues including germline tissues (ovaries, testes, and sperm) (Supplementary Figure 6A). Moreover, the transcript is abundant in early embryos (Supplementary Figure 6B), which are transcriptionally silent, suggesting that it is maternally deposited. In contrast to its target, propiR1 is not maternally deposited, but its expression becomes detectable by northern blot at around 5 hours post oviposition (Figure 7A). Initially, only the 30-nt isoform is expressed, but the 27-nt isoform becomes detectable 48 hours post oviposition (Figure 7A).

As *prop1R1* expression is maintained in most tissues in the adult mosquito (Supplementary Figure 6C), it is likely to have regulatory implications for other aspects of mosquito biology in adulthood. Yet, the dynamic regulation of *prop1R1* and its target *lnc027353* during embryogenesis prompted us to investigate the regulatory circuit in early development. Interestingly, we observed that the decrease of *lnc027353* expression coincided with onset of *prop1R1* expression (Figure 7B, Supplementary Figure 6B). To confirm that the reduction of *lnc027353* expression was *prop1R1* dependent we injected *Ae. aegypti* embryos with *prop1R1* AOs. Strikingly, this treatment resulted in a ~6-fold increase in *lnc027353* levels (Figure 7C), indicating *prop1R1* is indeed responsible for silencing *lnc027353* expression during early embryonic development.

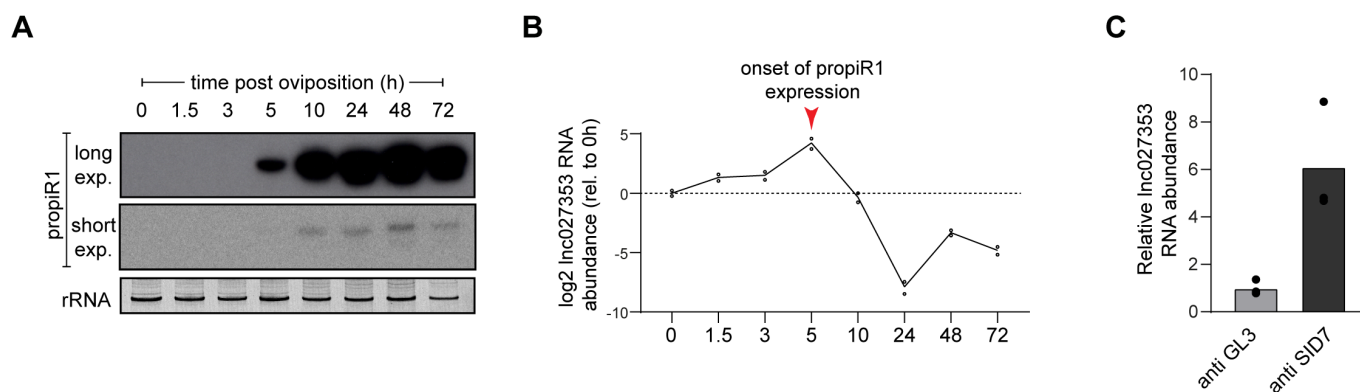


Figure 7. *prop1R1* regulates expression of *lnc027353* during early development.

A) Northern blot analysis of *prop1R1* in early embryonic development, with two different exposure times. Time indicates the age of the embryo in hours after a 30-minute egg laying (oviposition) period. For each time point, RNA from 200-400 eggs was pooled. EtBr stained rRNA serves as loading control. Northern blot was already used in (Halbach, 2020), and re-probed with a *prop1R1* probe.

B) *lnc027353* expression in early embryonic development corresponding to the northern blot in panel (A), as measured by RT-qPCR. Line and dots represent mean and individual measurements of two technical replicates, respectively. Expression was normalized to the 0h time point.

C) *lnc027353* expression in embryos injected with *prop1R1* or control AOs, as measured by RT-qPCR. Per condition, ~50 embryos were pooled. A representative of three independent experiments is shown. Bars and dots indicate the mean and individual measurements, respectively.

DISCUSSION

In *Ae. aegypti*, the PIWI gene family has undergone expansion to seven members, whereas the genetic model organism *Drosophila melanogaster* only encodes three. This expansion, together with the fact that PIWI proteins are expressed in somatic as well as germline tissues suggests that the piRNA pathway has gained additional functions in *Aedes* mosquitoes, aside from the repression of transposon in the germline. It has been proposed that the *Ae. aegypti* piRNA pathway is involved in various processes including antiviral defense, regulation of histone genes and degradation of maternally provided transcripts during maternal to zygotic transition (Girardi et al., 2017, Halbach, 2020, Miesen et al., 2015, Morazzani, Wiley et al., 2012, Schnettler, Donald et al., 2013, Tassetto, Kunitomi et al., 2019, Vodovar et al., 2012).

To reveal further non-canonical functions of the piRNA pathway in *Ae. aegypti*, we identified highly abundant endogenous piRNAs not originating from transposable elements. We found that one of these piRNAs (*prop1R1*) has strong silencing potential, and set out to characterize its function. In *Ae. aegypti* Aag2 cells, *prop1R1* is expressed as two isoforms (27 and 30 nt) which are differentially associated with Piwi4 and Piwi5. *prop1R1*-mediated target silencing requires Watson-Crick base pairing in the seed region plus additional

supplemental pairing at the 3' end. Given these lenient target sequence requirements, it was somewhat surprising that *prop1R1* strongly silences only a single target in Aag2 cells: *Inc027353*. It should be noted however that, given its ubiquitous expression both during development and in various adult mosquito tissues, *prop1R1* may have additional targets *in vivo*, that may not be expressed in Aag2-cells. *prop1R1* mediates silencing of *Inc027353* during early embryonic development and *prop1R1*-mediated cleavage results in the production of responder and trailer piRNAs from the cleavage fragment. Additionally, we show that the regulatory circuit consisting of *prop1R1* and *Inc027353* is conserved in *Ae. albopictus*, which implies its importance for mosquito development. Together, our results illustrate an intriguing interplay between a single piRNA, two PIWI proteins, and a lncRNA during embryonic development of *Aedes* mosquitoes.

Piwi4 and Piwi5 compete for a putative prop1R1 precursor

It has been hypothesized that members of the expanded PIWI gene family have specialized to preferentially process different RNA substrates (Lewis et al., 2016, Miesen et al., 2015, Miesen, Joosten et al., 2016). Apart from differences in the origin of RNA substrates that are processed into piRNAs, the spectrum of downstream mRNA targets might also vary based on differences in targeting requirements between PIWI proteins. The fact that *prop1R1* associates with two PIWI proteins (*Piwi4* and *Piwi5*) allowed us to investigate variations in the targeting requirements of two PIWI proteins guided by the same small RNA.

We found that silencing of reporters with a fully complementary *prop1R1* target site is reduced upon *Piwi5* knockdown, demonstrating that silencing of such targets is *Piwi5*-dependent. In line with this, reporters bearing a fully complementary target site are silenced more efficiently in *Piwi4* knockdown, most probably due to an increased availability of the *prop1R1* substrate to be processed into *Piwi5*-bound piRNAs. In contrast, *Piwi4* knockdown alleviated silencing of the *Inc027353* target gene as well as reporters containing the *Inc027353* target site, which contains mismatches at positions t10-15, t24-25 and t30. These results indicate that silencing of a fully complementary *prop1R1*-target site is achieved predominantly by *Piwi5*, whereas targeting of the imperfect target site in *Inc027353* results in *Piwi4*-mediated target repression.

Piwi5 is known to have slicing activity, as is evident from its involvement in the ping-pong amplification loop (Joosten et al., 2019, Miesen et al., 2015). Slicing-mediated target silencing is expected to require more extensive base pairing compared to slicing-independent silencing mechanisms (Reuter, Berninger et al., 2011) and therefore, it is expected that *Piwi5*-mediated silencing only allows a limited number of mismatches. Surprisingly, the production of responder and trailer piRNAs from the *Inc027353* cleavage fragment illustrates that the transcript is (at least in part) silenced through slicing, despite the fact that the *prop1R1* target site in *Inc027353* contains mismatches at the putative slice site. The exact sequence requirements necessary to accommodate slicing and subsequent responder piRNA production remain hitherto unexplored.

As previously observed for the *tapiR1*-*Piwi4* complex (Halbach, 2020), *prop1R1*/*Piwi4*-mediated targeting appears to be more 'miRNA-like' and likely requires the recruitment of accessory protein complexes to

establish slicing-independent target silencing. Despite extensive investigation (Halbach, 2020), the molecular machinery that is recruited to achieve Piwi4-mediated target silencing remains enigmatic.

Our study uncovered that propiR1/Piwi4 complexes do not require full sequence complementarity to silence target transcripts. Accordingly, when only piRNA-target duplexes with a limited number of mismatches are considered in bioinformatic predictions, a number of biological relevant small RNA targets may be missed. The targeting requirements of distinct PIWI protein complexes should therefore be more thoroughly characterized to inform piRNA target predictions.

As Piwi4 and Piwi5 have disparate spatiotemporal expression profiles (Akbari et al., 2013, Danet, Beauclair et al., 2019, Matthews, McBride et al., 2016, Wang, Jin et al., 2018), they may enforce propiR1-mediated regulation of various biological processes, thus expanding the regulatory potential of propiR1. It remains to be explored to what extent other piRNAs employ multiple PIWI-proteins in the regulation of host genes.

The propiR1-Inc027353 regulatory network in embryonic development

The target of propiR1, Inc027353, is a maternally provided transcript that is degraded during the first hours of embryonic development. This reduction in Inc027353 RNA levels coincides with an increase in propiR1 abundance and blocking propiR1 function with antisense oligonucleotides resulted in stabilization of the Inc027353 transcript, confirming that propiR1 is indeed responsible for Inc027353 degradation. While Piwi4 is maternally provided, Piwi5 expression commences later in embryonic development, after zygotic genome activation (Akbari et al., 2013). This is in line with the appearance of the distinct propiR1 isoforms during embryonic development, since the Piwi4-associated 30-nt isoform is already detectable at 5 hours post oviposition, whereas the Piwi5-associated 27-nt isoform appears only after 48 hours. Hence, it is likely that Inc027353 degradation is achieved by an accessory complex deposited by propiR1-guided Piwi4. This does not, however, rule out a role for Piwi5 in Inc027353 regulation at later stages of embryonic development in other life stages of the mosquito.

The importance of piRNAs during embryonic development is supported by the fact that piRNA levels peak during embryonic development (Liu, Dong et al., 2016), and by their involvement in the degradation of maternal transcripts during MZT (Barckmann et al., 2015, Halbach, 2020, Rouget et al., 2010). We hypothesize that the observed lncRNA degradation induced by propiR1 in *Aedes* mosquitoes is essential for embryonic development, however, the exact function of Inc027353 remains to be explored.

Evolutionary conservation of the network

We found that *Ae. albopictus* also expresses propiR1 and a putative Inc027353 orthologue in which the sequence adjacent to the propiR1 target site is preferentially conserved. The high degree of sequence conservation of especially the target site suggests that this genomic region has important functions that have been maintained under evolutionary pressure. Although not annotated as a repeat, propiR1 is encoded by seven and ten repetitive loci in *Ae. aegypti* and *Ae. albopictus*, respectively. Notably, propiR1 contains a single

nucleotide deletion in *Ae. albopictus* compared to the *Ae. aegypti* sequence. Since all propiR1 loci in *Ae. albopictus* share this deletion, the most parsimonious interpretation is that the genome of the common ancestor of *Ae. aegypti* and *Ae. albopictus* contained a single propiR1 locus, which has duplicated independently in both species.

Our newly discovered regulatory circuit in which propiR1 targets and degrades a single lncRNA target illustrates an intriguing non-canonical role for the piRNA pathway. The conservation of propiR1 as well as its target site in the homologue of lnc027353 in *Ae. albopictus*, together with its role during early embryonic development suggests that the circuit is crucial for mosquito development. propiR1 is one of millions of different piRNA sequences (Arensburger et al., 2011), which may differ in their spatiotemporal expression patterns. Hence, the gene-regulatory potential of the *Aedes* piRNA pathway is likely to be highly complex and many interesting regulatory circuits remain to be explored.

MATERIAL AND METHODS

Cell culture

Aedes aegypti Aag2 cells and *Aedes albopictus* U4.4 cells were grown at 27°C in Leibovitz's L-15 medium (Invitrogen) supplemented with 10% fetal bovine serum (Gibco), 2% tryptose phosphate broth (Sigma), 50 U/mL Penicillin, 50µg/mL Streptomycin (Gibco), and 1% Non-essential amino acids (Gibco).

Gene-knockdown using dsRNA

PCR products containing a T7 promoter sequence at both ends were generated and *in vitro* transcribed by T7 polymerase, heated to 80°C and gradually cooled down to form dsRNA. The dsRNA was purified using the GenElute Mammalian Total RNA kit (Sigma). Primers that were used to generate double stranded RNA are described in (Miesen et al., 2015)

For knockdown experiments, cells were seeded at $\sim 1 \times 10^5$ cells/well in a 24-well plate and allowed to attach overnight. On the following day, 150 ng dsRNA/well was transfected into cells using 0.6 µL X-tremeGENE HP DNA Transfection Reagent (Sigma) according to the manufacturer's instructions. Three hours later, medium was replaced by fresh, supplemented L15-medium. To improve knockdown efficiency, cells were transfected again in the same way 48 hours after the initial knockdown. 48 hours after the second transfection, cells were harvested in 1mL RNA-Solv Reagent (Omega Bio-Tek) for RNA isolation.

RNA isolation

Cells were thoroughly homogenized in 1 mL RNA-Solv Reagent and subsequently, 200 µL of chloroform was added. After harsh vortexing and centrifugation, the aqueous phase was collected and RNA was precipitated in 1.5 volumes of isopropanol for ~ 30 minutes on ice. RNA was pelleted by spinning at $\sim 18000 \times g$ for 30 minutes at 4°C. Subsequently, pellets were washed 2-3 times in 85% ethanol and dissolved in nuclease free water.

Periodate treatment and β -elimination

3' modification of propiR1 was analyzed by re-probing a northern blot previously used in (Halbach, 2020) with a propiR1 probe. For comparative reasons, the miR2940-3p blot is shown here again.

Small RNA Northern blot

5-10 µg RNA was diluted in 2x RNA loading dye (New England Biolabs) and size separated on 7 M UREA/15% polyacrylamide/0.5xTBE gels by gel electrophoresis. RNA was transferred to Hybond Nx nylon membranes (Amersham) and crosslinked using EDC (1-ethyl-3-(3-dimethylaminopropyl)carbodiimide hydrochloride) (Sigma). Membranes were pre-hybridized in Ultrahyb Oligo hybridization buffer (Invitrogen), after which ^{32}P labeled DNA oligonucleotides were added for overnight hybridization at 42°C. Membranes were washed 10 minutes in 2xSSC/0.1% SDS followed by 20 minutes in 1xSSC/0.1% SDS at 42°C. Kodak XAR X-ray films

were exposed to radiolabeled membranes and developed using an Agfa CP1000 developer. Northern blots shown in Fig. 7A and Supplementary Fig 6C have already been used in (Halbach, 2020), and were re-probed with a propiR1 probe. The rRNA image is shown here again as loading control.

Probes used for northern blotting were:

propiR1	ATCAATTTTGCAAATTGTAAGTCGTATGTC
U6 snRNA	GATTTTGCGTGTTCATCCTTGTGCAGGGGCCATGCTAA
miR2940-3p	AGTGATTTATCTCCCTGTGCGAC
Inc027353-responder	GATACATTTCTACAAAATTAGACATACGAA

Immunoprecipitation of PIWI proteins

Generation and characterization of anti-PIWI antibodies was described in (Joosten et al., 2019) and (Halbach, 2020) and immunoprecipitation was performed as described in (Joosten et al., 2019).

Analysis of sequence conservation

Multiple sequence alignments (MSA) of DNA sequences were generated with ClustalW (<https://www.genome.jp/tools-bin/clustalw>) with default settings. Conservation scores for seven *Aedes aegypti* propiR1 sites plus 0.5 kb flanking regions were calculated using the consurf server (<http://consurf.tau.ac.il/>) (Ashkenazy, Abadi et al., 2016) using the following settings: nucleotide sequence, no structure, MSA upload, no tree, Bayesian calculation method, Best evolutionary model. The conservation scores and the corresponding borders of the 50% confidence interval from the output file were multiplied by -1 to display higher conservation by increasing values and subsequently a sliding window analysis was applied. The mean of five consecutive nucleotide positions with an offset of one position was plotted.

Reporter cloning

To generate reporter constructs, a pMT-GL3 vector, encoding firefly luciferase (GL3) under control of a copper sulphate (CuSO₄)-inducible metallothionein promoter (pMT) (van Rij, Saleh et al., 2006), was digested with *Pme*I and *Sac*II restriction enzymes for 3 - 4 hours at 37°C and dephosphorylated using Antarctic Phosphatase (NEB) for 1 hour at 37°C. To produce target site inserts, sense and antisense DNA oligonucleotides (50 µM) containing various propiR1 target sites (Supplementary Table S1) were heated at 90°C for 10 minutes in 100 mM Tris-HCl (pH 7.5), 0.1 M NaCl, 10 mM EDTA before gradually cooling to room temperature to anneal the oligonucleotides. Inserts were subsequently phosphorylated for 30 minutes at 37°C using T4 polynucleotide kinase (Roche). 5 µL of 25 × diluted oligonucleotides and 50ng of the digested and dephosphorylated vector were ligated overnight at 16°C using T4 Ligase (Roche), and transformed into XL10-Gold *E. coli*. Plasmid DNA was isolated using the High Pure Plasmid Isolation kit (Roche). Sequences were confirmed by Sanger sequencing.

Luciferase assay

Approximately 2×10^4 Aag2 cells/well were seeded in 96-well plates and incubated overnight. Per well, 100 ng of the pMT-GL3 reporter construct and 100 ng of pMT-*Renilla* Luciferase plasmid (van Rij et al., 2006) was transfected using 0.2 μ L X-tremeGENE HP DNA, according to manufacturer's instructions. To induce the metallothionein promoter of the reporter constructs, medium was replaced with fully supplemented Leibovitz's L-15 medium containing 0.5 mM CuSO₄ 3 to 4 hours after transfection. In case of luciferase experiments in PIWI-depleted cells, reporter constructs were co-transfected with PIWI dsRNA during the second knockdown. In experiments in which PIWI-mediated silencing was blocked by antisense oligonucleotides (AOs), 100 ng of the FLuc reporters and 100 ng pMT-*Renilla* Luciferase were co-transfected with indicated concentrations of 5' Cy5-labelled, fully 2'-O-methylated AOs using 4 μ L X-tremeGENE HP DNA transfection reagent per 1 μ g of oligonucleotides. 24 hours after activation of the metallothionein promoters, cells were lysed in 30 μ L Passive lysis buffer (Promega) per well. The activity of *Renilla* and firefly luciferase was measured using the Dual Luciferase Reporter Assay system (Promega) on a Modulus Single Tube Reader (Turner Biosystems). For each well, firefly luciferase was normalized to *Renilla* luciferase activity.

mRNA-seq analysis

Reads were mapped to the *Aedes aegypti* LVP_AGWG AaegL5.1 reference genome obtained from VectorBase (<https://www.vectorbase.org/>) and quantified with STAR aligner (version 2.5.2b) (Dobin, Davis et al., 2013) in 2-pass mode. Briefly, all libraries were first mapped with options `--readFilesCommand zcat --outSAMtype None --outSAMattrIHstart 448 0 --outSAMstrandField intronMotif`, then all detected splice junctions were combined (false positive junctions on the mitochondrial genome were removed), and used in a second mapping step with `-sjdbFileChrStartEnd`, other parameters as above, and `-quantMode GeneCounts` in order to quantify gene expression. Transposons were quantified with Salmon (v.0.8.2) (Patro, Duggal et al., 2017) on the TEfam transposon consensus sequence (<https://tefam.biochem.vt.edu/tefam/>, accessed April 2017) with default settings and libType set to "ISR". Statistical analyses were performed with DEseq2 (Love, Huber et al., 2014) and significance was tested at an FDR of 0.01 and a log₂ fold change of 0.5. Results were plotted in R with ggplot2 (Wickham, 2009).

For Figures 6A-B, publicly available datasets were obtained from Sequence Read Archive (SRA, <https://www.ncbi.nlm.nih.gov/sra>) and mapped and quantified with STAR aligner as described above. Normalization factors were estimated with DEseq2, and normalized counts were plotted with ggplot2. A list of datasets used can be found in Supplementary table S2.

sRNA-seq analysis

3' sequencing adapters were clipped from sRNA sequencing reads with Cutadapt (version 1.14) (Martin, 2011) (options `-m 15 -M 35 --discard-untrimmed`), that were subsequently mapped to the AaegL5.1 reference genome with Bowtie (version 0.12.17) (Langmead, Trapnell et al., 2009) without allowing mismatches (options

--best -k 1 -v 0). Reads were trimmed to the first 25 nt to include different isoforms of a given piRNA, IP libraries (Miesen et al., 2015) were normalized to total mapped small RNA reads per million, and enrichment of piRNAs was then calculated as log2 fold enrichment compared to a GFP-control IP. For Fig. 1A, piRNAs as least twofold enriched in Piwi5 were filtered by their average abundance in triplicate control FLuc knockdown libraries from total small RNAs in Aag2 cells (Miesen et al., 2015), and overlapped with annotated transposable elements obtained from VectorBase with bedtools intersect (Quinlan, 2014). Coverage of the AAEL027353 target locus and of the propiR1 loci were determined with bedtools coverage (Quinlan, 2014), normalized to miRNA reads per million, and plotted in R with Gviz (Hahne, 2016) Size distribution of propiR1 small RNAs in *Ae. aegypti* Aag2 and *Ae. albopictus* U4.4 cells were generated from the control knockdown condition from (Miesen et al., 2015) and from a small RNA sequencing library obtained from untreated U4.4 cells (PRJNA613255). Adapter sequences were clipped using the Clip adapter sequence tool (v1.03; options all default) within the public server of the usegalaxy.org instance (Afgan, Baker et al., 2018), and small RNA reads were subsequently mapped to the AaegL5.1 and the AalbF2 genome assemblies, respectively with Bowtie (version 0.12.17) (Langmead et al., 2009) without allowing mismatches (options: -n0 -I 32 -k 1). The read counts were normalized to the respective library size.

RT-qPCR

Cells were treated with AOs as described above. After RNA isolation, 0.5-1µg of total RNA was DNaseI treated (Ambion), reverse transcribed using the Taqman reverse transcription kit (Applied Biosystems), and SYBR-green qPCR was performed using the GoTaq qPCR system (Promega) according to manufacturer's recommendations. Expression levels of target genes were normalized to the expression of the housekeeping gene lysosomal aspartic protease (LAP) and fold changes in expression were calculated using the $2^{(-\Delta\Delta CT)}$ method (Livak & Schmittgen, 2001).

Mosquito rearing and egg laying

Aedes aegypti mosquitoes Liverpool strain were reared at 28 ± 1 °C, 80% humidity with a 12h:12h light: dark cycle. Eggs were hatched in tap water, and larvae were fed with fish food powder (Tetramin) every other day. Adults were allowed constant access to 10% (w/v) sucrose in water, and females were fed on human blood (Sanquin Blood Supply Foundation, Nijmegen, the Netherlands) through a membrane feeding system (Hemotek Ltd.). For injection experiments, females were separated, offered a blood meal, and allowed to lay eggs three to four days later by providing a moist surface and placing the mosquitoes in the dark. Embryos were collected at the indicated time-points after a 30 minute egg laying period. For Fig. 7A-B, *Ae. aegypti* Jane mosquitoes were used as described previously (Halbach 2020).

Statistical analyses

Unless noted otherwise, unpaired two tailed t-tests with Holm-Sidak correction for multiple comparisons were used to test statistical significance (* $P < 0.05$, ** $P < 0.005$, *** $P < 0.0005$).

ACKNOWLEDGEMENTS

We thank members of the laboratory for fruitful discussions, Bas Pennings for technical assistance in cloning of luciferase reporters, and Prof. Martijn Huijnen from the Center for Molecular and Biomolecular Informatics (CMBI) Nijmegen for bioinformatics advice. Sequencing was performed by the GenomEast platform, a member of the “France Génomique” consortium (ANR-10-INBS-0009). This work was financially supported by a fellowship from the Radboud University Medical Center, a Consolidator Grant from the European Research Council (ERC) under the European Union’s Seventh Framework Programme (ERC CoG grant number 615680), and a VICI grant from the Netherlands Organization for Scientific Research (grant number 016.VICI.170.090). *Ae. aegypti* Liverpool strain mosquitoes were kindly provided by the NIH/NIAID Filariasis Research Reagent Resource Center, distributed by BEI Resources, NIAID, NIH.

AUTHOR CONTRIBUTIONS

VB, JJ and RH designed and performed experiments. RH performed the embryo injections. MT generated and analyzed some of the luciferase reporters. RH and PM conducted bio-informatic analyses. RvR conceived the study and acquired funding. JJ, VB, and RvR wrote the manuscript with input from all other authors.

CONFLICT OF INTEREST

The authors declare that they have no conflict of interest.

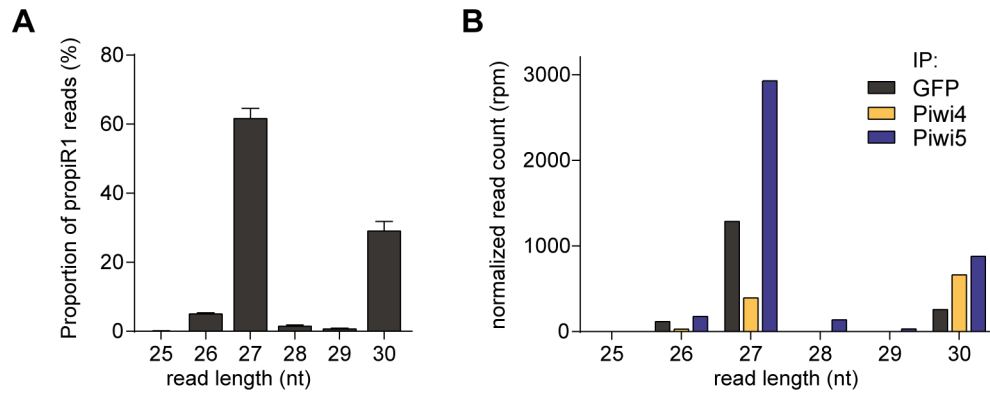
REFERENCE LIST

- Afgan E, Baker D, Batut B, van den Beek M, Bouvier D, Cech M, Chilton J, Clements D, Coraor N, Gruning BA, Guerler A, Hillman-Jackson J, Hiltmann S, Jalili V, Rasche H, Soranzo N, Goecks J, Taylor J, Nekrutenko A, Blankenberg D (2018) The Galaxy platform for accessible, reproducible and collaborative biomedical analyses: 2018 update. *Nucleic acids research* 46: W537-W544
- Akbari OS, Antoshechkin I, Amrhein H, Williams B, Diloreto R, Sandler J, Hay BA (2013) The developmental transcriptome of the mosquito *Aedes aegypti*, an invasive species and major arbovirus vector. *G3 (Bethesda)* 3: 1493-509
- Arensburger P, Hice RH, Wright JA, Craig NL, Atkinson PW (2011) The mosquito *Aedes aegypti* has a large genome size and high transposable element load but contains a low proportion of transposon-specific piRNAs. *Bmc Genomics* 12
- Ashkenazy H, Abadi S, Martz E, Chay O, Mayrose I, Pupko T, Ben-Tal N (2016) ConSurf 2016: an improved methodology to estimate and visualize evolutionary conservation in macromolecules. *Nucleic acids research* 44: W344-50
- Brennecke J, Aravin AA, Stark A, Dus M, Kellis M, Sachidanandam R, Hannon GJ (2007) Discrete small RNA-generating loci as master regulators of transposon activity in *Drosophila*. *Cell* 128: 1089-1103
- Campbell CL, Black WC, Hess AM, Foy BD (2008) Comparative genomics of small RNA regulatory pathway components in vector mosquitoes. *Bmc Genomics* 9
- Danet L, Beauclair G, Berthet M, Moratorio G, Gracias S, Tangy F, Choumet V, Jouvenet N (2019) Midgut barriers prevent the replication and dissemination of the yellow fever vaccine in *Aedes aegypti*. *PLoS neglected tropical diseases* 13: e0007299
- Dobin A, Davis CA, Schlesinger F, Drenkow J, Zaleski C, Jha S, Batut P, Chaisson M, Gingeras TR (2013) STAR: ultrafast universal RNA-seq aligner. *Bioinformatics* 29: 15-21
- Girardi E, Miesen P, Pennings B, Frangeul L, Saleh MC, van Rij RP (2017) Histone-derived piRNA biogenesis depends on the ping-pong partners Piwi5 and Ago3 in *Aedes aegypti*. *Nucleic acids research* 45: 4881-4892
- Gunawardane LS, Saito K, Nishida KM, Miyoshi K, Kawamura Y, Nagami T, Siomi H, Siomi MC (2007) A slicer-mediated mechanism for repeat-associated siRNA 5' end formation in *Drosophila*. *Science* 315: 1587-90
- Hahne FI, R. (2016) Visualizing Genomic Data Using Gviz and Bioconductor. *Methods in molecular biology* 1418: 335-351
- Halbach RM, P.; Joosten, J.; Taşköprü, E.; Pennings, B.; Vogels, CBF.; Merklng, SH.; Koenraadt, CJ.; Lambrechts L.; van Rij, RP. (2020) An ancient satellite repeat controls gene expression and embryonic development in *Aedes aegypti* through a highly conserved piRNA. *BioRxiv*
- Horwich MD, Li C, Matranga C, Vagin V, Farley G, Wang P, Zamore PD (2007) The *Drosophila* RNA methyltransferase, DmHen1, modifies germline piRNAs and single-stranded siRNAs in RISC. *Current biology* : CB 17: 1265-72
- Joosten J, Miesen P, Taskopru E, Pennings B, Jansen P, Huynen MA, Vermeulen M, Van Rij RP (2019) The Tudor protein Veneno assembles the ping-pong amplification complex that produces viral piRNAs in *Aedes* mosquitoes. *Nucleic acids research* 47: 2546-2559
- Kawaoka S, Katsuma S, Tomari Y (2014) Making piRNAs in vitro. *Methods in molecular biology* 1093: 35-46
- Kobayashi H, Tomari Y (2016) RISC assembly: Coordination between small RNAs and Argonaute proteins. *Bba-Gene Regul Mech* 1859: 71-81
- Langmead B, Trapnell C, Pop M, Salzberg SL (2009) Ultrafast and memory-efficient alignment of short DNA sequences to the human genome. *Genome biology* 10: R25
- Lewis SH, Quarles KA, Yang YJ, Tanguy M, Frezal L, Smith SA, Sharma PP, Cordaux R, Gilbert C, Giraud I, Collins DH, Zamore PD, Miska EA, Sarkies P, Jiggins FM (2018) Pan-arthropod analysis reveals somatic piRNAs as an ancestral defence against transposable elements. *Nat Ecol Evol* 2: 174-181
- Lewis SH, Salmela H, Obbard DJ (2016) Duplication and Diversification of Dipteran Argonaute Genes, and the Evolutionary Divergence of Piwi and Aubergine. *Genome Biol Evol* 8: 507-518
- Liu P, Dong Y, Gu J, Puthiyakunnon S, Wu Y, Chen XG (2016) Developmental piRNA profiles of the invasive vector mosquito *Aedes albopictus*. *Parasites & vectors* 9: 524

- Livak KJ, Schmittgen TD (2001) Analysis of relative gene expression data using real-time quantitative PCR and the 2(-Delta Delta C(T)) Method. *Methods* 25: 402-8
- Love MI, Huber W, Anders S (2014) Moderated estimation of fold change and dispersion for RNA-seq data with DESeq2. *Genome biology* 15: 550
- Martin M (2011) Cutadapt removes adapter sequences from high-throughput sequencing reads. *EMBnetjournal* 17: pg. 10-12
- Matsumoto N, Nishimasu H, Sakakibara K, Nishida KM, Hirano T, Ishitani R, Siomi H, Siomi MC, Nureki O (2016) Crystal Structure of Silkworm PIWI-Clade Argonaute Siwi Bound to piRNA. *Cell* 167: 484-497 e9
- Matthews BJ, McBride CS, DeGennaro M, Despo O, Vosshall LB (2016) The neurotranscriptome of the *Aedes aegypti* mosquito. *Bmc Genomics* 17: 32
- Miesen P, Girardi E, van Rij RP (2015) Distinct sets of PIWI proteins produce arbovirus and transposon-derived piRNAs in *Aedes aegypti* mosquito cells. *Nucleic acids research* 43: 6545-56
- Miesen P, Joosten J, van Rij RP (2016) PIWIs Go Viral: Arbovirus-Derived piRNAs in Vector Mosquitoes. *PLoS Pathog* 12: e1006017
- Mohn F, Handler D, Brennecke J (2015) piRNA-guided slicing specifies transcripts for Zucchini-dependent, phased piRNA biogenesis. *Science* 348: 812-817
- Morazzani EM, Wiley MR, Murreddu MG, Adelman ZN, Myles KM (2012) Production of virus-derived ping-pong-dependent piRNA-like small RNAs in the mosquito soma. *PLoS Pathog* 8: e1002470
- Ozata DM, Gainetdinov I, Zoch A, O'Carroll D, Zamore PD (2019) PIWI-interacting RNAs: small RNAs with big functions. *Nat Rev Genet* 20: 89-108
- Palatini U, Miesen P, Carballar-Lejarazu R, Ometto L, Rizzo E, Tu ZJ, van Rij RP, Bonizzoni M (2017) Comparative genomics shows that viral integrations are abundant and express piRNAs in the arboviral vectors *Aedes aegypti* and *Aedes albopictus*. *Bmc Genomics* 18
- Patro R, Duggal G, Love MI, Irizarry RA, Kingsford C (2017) Salmon provides fast and bias-aware quantification of transcript expression. *Nature methods* 14: 417-419
- Quinlan AR (2014) BEDTools: The Swiss-Army Tool for Genome Feature Analysis. *Current protocols in bioinformatics* 47: 11 12 1-34
- Rehmsmeier M, Steffen P, Hochsmann M, Giegerich R (2004) Fast and effective prediction of microRNA/target duplexes. *Rna* 10: 1507-17
- Reuter M, Berninger P, Chuma S, Shah H, Hosokawa M, Funaya C, Antony C, Sachidanandam R, Pillai RS (2011) Miwi catalysis is required for piRNA amplification-independent LINE1 transposon silencing. *Nature* 480: 264-U154
- Rouget C, Papin C, Boureux A, Meunier AC, Franco B, Robine N, Lai EC, Pelisson A, Simonelig M (2010) Maternal mRNA deadenylation and decay by the piRNA pathway in the early *Drosophila* embryo. *Nature* 467: 1128-32
- Saito K, Sakaguchi Y, Suzuki T, Suzuki T, Siomi H, Siomi MC (2007) Pimet, the *Drosophila* homolog of HEN1, mediates 2'-O-methylation of Piwi-interacting RNAs at their 3' ends. *Genes & development* 21: 1603-8
- Schnettler E, Donald CL, Human S, Watson M, Siu RW, McFarlane M, Fazakerley JK, Kohl A, Fragkoudis R (2013) Knockdown of piRNA pathway proteins results in enhanced Semliki Forest virus production in mosquito cells. *J Gen Virol* 94: 1680-9
- Shen EZ, Chen H, Ozturk AR, Tu S, Shirayama M, Tang W, Ding YH, Dai SY, Weng Z, Mello CC (2018) Identification of piRNA Binding Sites Reveals the Argonaute Regulatory Landscape of the *C. elegans* Germline. *Cell* 172: 937-951 e18
- Suzuki Y, Frangeul L, Dickson LB, Blanc H, Verdier Y, Vinh J, Lambrechts L, Saleh MC (2017) Uncovering the Repertoire of Endogenous Flaviviral Elements in *Aedes* Mosquito Genomes. *J Virol* 91
- Tadros W, Lipshitz HD (2009) The maternal-to-zygotic transition: a play in two acts. *Development* 136: 3033-42
- Tassetto M, Kunitomi M, Whitfield ZJ, Dolan PT, Sánchez-Vargas I, Garcia-Knight M, Ribiero I, Chen T, Olson KE, Andino R (2019) Control of RNA viruses in mosquito cells through the acquisition of vDNA and endogenous viral elements. *eLife* 8: e41244

- Tian Y, Simanshu DK, Ma JB, Patel DJ (2011) Structural basis for piRNA 2'-O-methylated 3'-end recognition by Piwi PAZ (Piwi/Argonaute/Zwille) domains. *Proceedings of the National Academy of Sciences of the United States of America* 108: 903-10
- Vagin VV, Sigova A, Li CJ, Seitz H, Gvozdev V, Zamore PD (2006) A distinct small RNA pathway silences selfish genetic elements in the germline. *Science* 313: 320-324
- van Rij RP, Saleh MC, Berry B, Foo C, Houk A, Antoniewski C, Andino R (2006) The RNA silencing endonuclease Argonaute 2 mediates specific antiviral immunity in *Drosophila melanogaster*. *Genes & development* 20: 2985-2995
- Vodovar N, Bronkhorst AW, van Cleef KW, Miesen P, Blanc H, van Rij RP, Saleh MC (2012) Arbovirus-derived piRNAs exhibit a ping-pong signature in mosquito cells. *PLoS one* 7: e30861
- Vourekas A, Alexiou P, Vrettos N, Maragkakis M, Mourelatos Z (2016) Sequence-dependent but not sequence-specific piRNA adhesion traps mRNAs to the germ plasm. *Nature* 531: 390-394
- Wang Y, Jin B, Liu P, Li J, Chen X, Gu J (2018) piRNA Profiling of Dengue Virus Type 2-Infected Asian Tiger Mosquito and Midgut Tissues. *Viruses* 10
- Watanabe T, Cheng EC, Zhong M, Lin H (2015) Retrotransposons and pseudogenes regulate mRNAs and lncRNAs via the piRNA pathway in the germline. *Genome Res* 25: 368-80
- Whitfield ZJ, Dolan PT, Kunitomi M, Tassetto M, Seetin MG, Oh S, Heiner C, Paxinos E, Andino R (2017) The Diversity, Structure, and Function of Heritable Adaptive Immunity Sequences in the *Aedes aegypti* Genome. *Current biology* : CB 27: 3511-3519 e7
- Wickham H (2009) *Ggplot2 : elegant graphics for data analysis*. Springer, New York
- Yamaguchi S, Oe A, Nishida KM, Yamashita K, Kajiya A, Hirano S, Matsumoto N, Dohmae N, Ishitani R, Saito K, Siomi H, Nishimasu H, Siomi MC, Nureki O (2020) Crystal structure of *Drosophila* Piwi. *Nat Commun* 11: 858

Supplementary Figure 1.



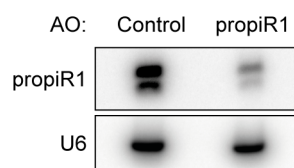
Supplementary Figure 1. Size distribution of propiR1 isoforms in *Ae. aegypti*.

A) Size distribution of propiR1 reads in small RNA deep sequencing libraries generated from dsLuc-treated Aag2 cells. The datasets used here [also (B)] were first described in (Miesen et al., 2015).

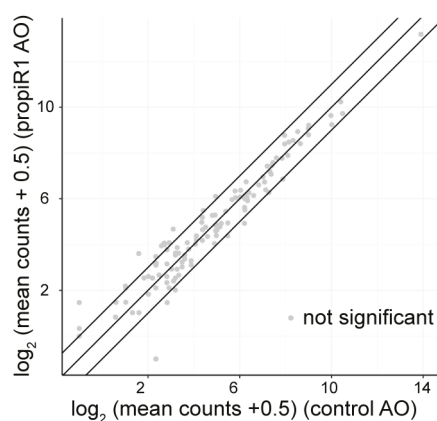
B) Size distribution of propiR1 isoforms in immunoprecipitations (IP) of Piwi4 and Piwi5. GFP-IP serves as non-specific background binding control. Read count is normalized to library size.

Supplementary Figure 3

A



B



C

AAEL027353-RA
mfe: -29.4 kcal/mol

```
target 5' U GC GGCAAU U 3'
        UCGG UUGCAGAU UCGUAUGUC
        ||||| |||||
        AGUU AACGUUUA AGCAUACAG
prop1R1 3' U AA ACAUUC 5'
```

AAEL001794-RB
mfe: -23.6 kcal/mol

```
target 5' A CUCACCG C 3'
        CGGUUUUGCG CGUAUGUU
        ||||| |||||
        GUUAAAACGU GCAUACAG
prop1R1 3' UA UUAACAUUCA 5'
```

AAEL000564-RH
mfe: -26.3 kcal/mol

```
target 5' A CAUCAAU A 3'
        GCAG GGUCGUAUGUC
        ||||| |||||
        CGUU UCAGCAUACAG
prop1R1 3' UAGUUAAAA UAACAU 5'
```

AAEL009838-RA
mfe: -25.9 kcal/mol

```
target 5' U GCUCGUC UC GAGUAU A A 3'
        UCAGUU UGC GGUUG AG UCGUGUGUU
        ||||| ||| ||||| || |||||
        AGUUUA ACG UUAAC UC AGCAUACAG
prop1R1 3' U A U AU 5'
```

AAEL006445-RA
mfe: -24.2 kcal/mol

```
target 5' U GG G CUGAUG GUUGGG A U 3'
        UCG UUUG G GAU GUGGG UUGUAUGUC
        ||| ||||| ||| ||||| |||||
        AGU AAAC U UUA CAUUC AGCAUACAG
prop1R1 3' U UA G A 5'
```

AAEL003865-RB
mfe: -24.4 kcal/mol

```
target 5' G CGA A AUCG GAA A 3'
        AUCA GCAGGU GU GAG GUAUGUC
        ||||| ||||| || |||||
        UAGU CGUUUA CA UUC CAUACAG
prop1R1 3' UAAAA A AG 5'
```

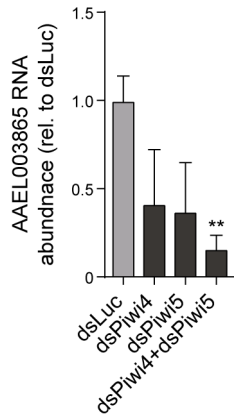
Supplementary Figure 3. Effect of propiR1 on transposable elements and predicted structures of propiR1-target duplexes.

A) Northern blot analysis of propiR1 abundance in Aag2 cells treated with 300nM propiR1 or control antisense oligonucleotides (AO) for 48 hours.

B) Log₂ expression of transposable elements in Aag2 cells treated with propiR1 or control AOs. Mean RNA-seq counts of three biological replicates are shown (plus a pseudo-count of 0.5 to plot values of zero). Significance was tested at an FDR of 0.01 and log₂ fold change of 0.5. Diagonal lines highlight a 2-fold change.

C) Schematic representation of predicted propiR1-target duplexes in indicated genes and their minimum free energy.

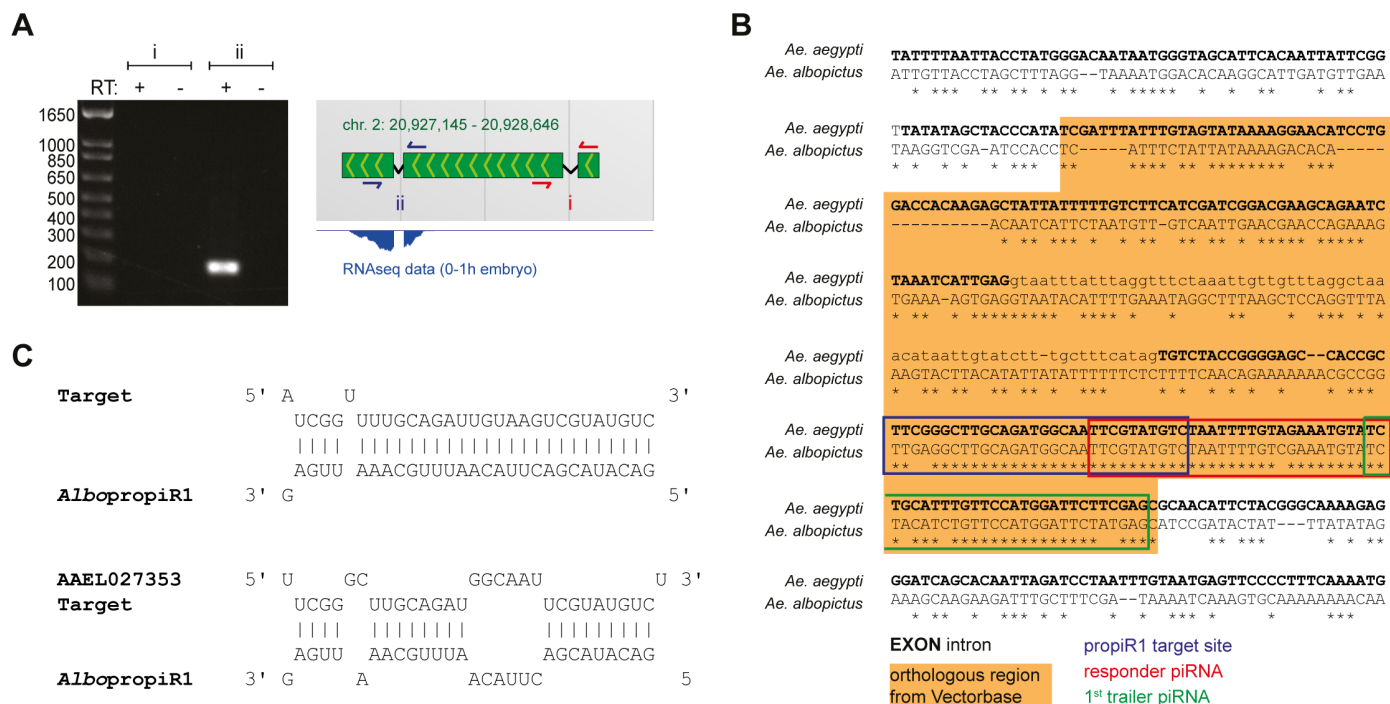
Supplementary Figure 4



Supplementary Figure 4. Expression of AAEL003865 upon Piwi4 and Piwi5 knockdown.

Relative expression of AAEL003865 upon Piwi4 and Piwi5 single and double knockdown in Aag2 cells, measured by RT-qPCR. dsLuc knockdown serves as a control. Piwi4 and Piwi5 knockdown resulted in decreased AAEL003865 expression (~2.4-fold and ~2.7-fold, respectively) and combined Piwi4 and Piwi5 knockdown resulted in a ~6.3-fold reduction of AAEL003865 expression. These results are in line with the finding that AAEL003865 expression was reduced upon propiR1 AO treatment (Figure 3B-C). Yet, as the propiR1 target site predicted in AAEL003865 did not affect luciferase activity in reporter assays (Figure 3E), propiR1 is unlikely to directly regulate AAEL003865 expression. Data depict the mean and standard deviation of three biological replicates. Asterisks denote statistically significant differences in AAEL003865 expression compared to dsLuc treated cells (unpaired two tailed t-tests with Holm-Sidak correction; ** $P < 0.005$)

Supplemental Figure 5.



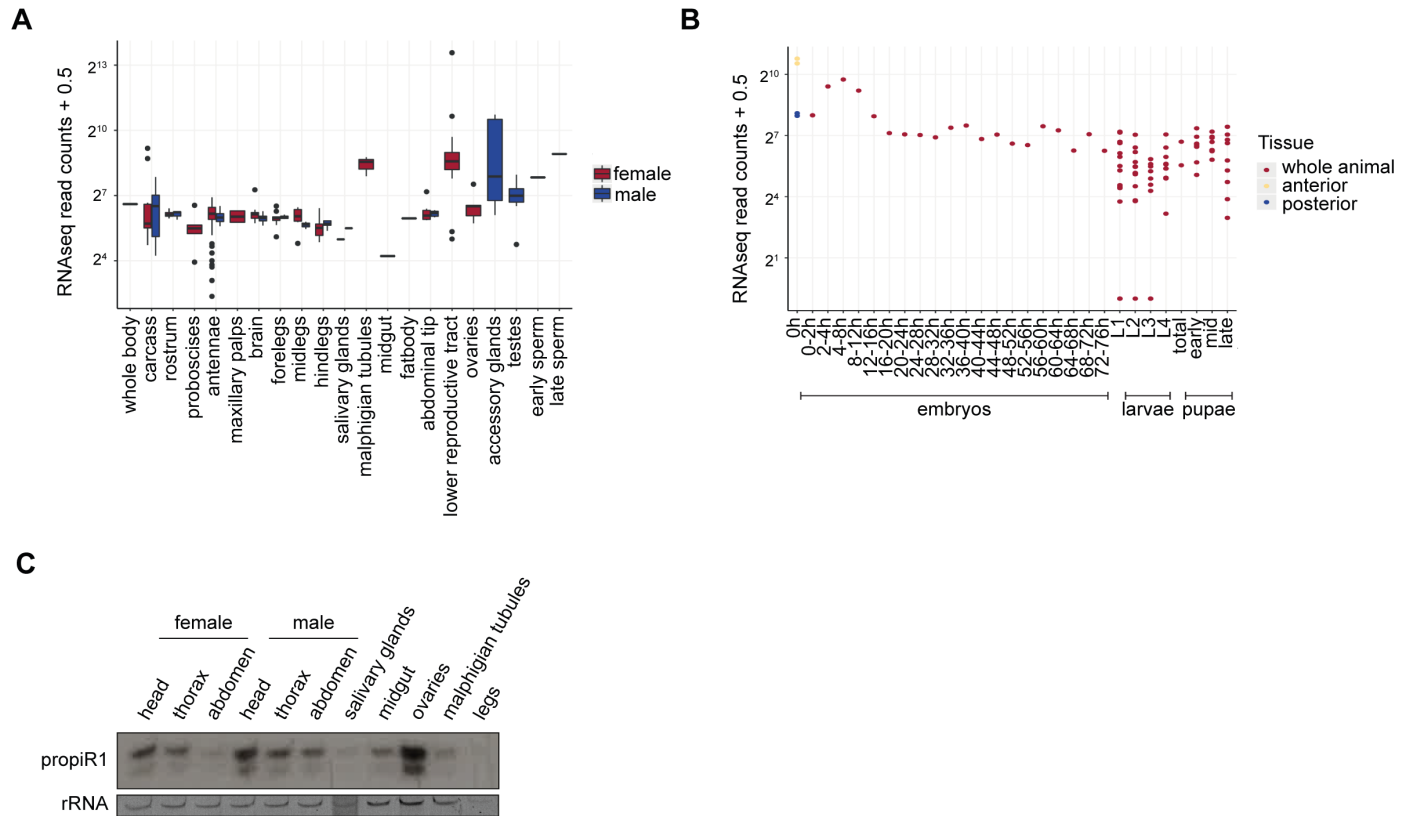
Supplementary Figure 5. Characterization of the *Ae. albopictus* Inc027353 orthologous sequence.

A) PCR on cDNA from Aag2 cells with primer pairs covering either the exon 1-2 junction (i) or exon 2-3 junction (ii) intron (primer location shown in the right panel). Reactions in the absence of reverse transcriptase were included as control, as indicated.

B) ClustalW alignment of *Ae. aegypti* Inc027353 and its *Ae. albopictus* ortholog. The yellow shaded area indicates a stretch that is annotated in VectorBase as an orthologous region. The propiR1 target site, responder piRNA, and the 1st trailer piRNA are indicated by blue, red and green boxes, respectively. Sequences annotated as exons are in uppercase bold font; intronic sequence is in lowercase regular font.

C) Schematic representation of piRNA-target duplexes involving *Ae. albopictus* propiR1 with the *Ae. aegypti* propiR1 fully complementary target site (upper panel) and the *Ae. aegypti* Inc027353 target site (lower panel), that were introduced in the FLuc reporter used in Figure 6D.

Supplementary Figure 6.



Supplementary Figure 6. Spatiotemporal expression of *Inc027353* and *propiR1*.

A-B) Expression of *Inc027353* across developmental stage (A) and in different tissues (B) of *Ae. aegypti*. Values are normalized RNA-seq counts with a pseudo-count of 0.5 added to plot values of zero.

C) Northern blot analysis of *propiR1* in different tissues of adult *Ae. aegypti*. EtBr stained rRNA serves as a loading control. Northern blot was published in (Halbach, 2020), and re-probed for *propiR1*.